Study environmental dependence of galaxy properties

Sergei Dodonov[1], Aleksandra Grokhovskaya[1]

[1] SAO RAS (Special Astrophysical Observatory)

12th Serbian Conference on Spectral Line Shapes in Astrophysics
Vrdnik, Serbia, June 3-7, 2019

The reasons

Galaxies

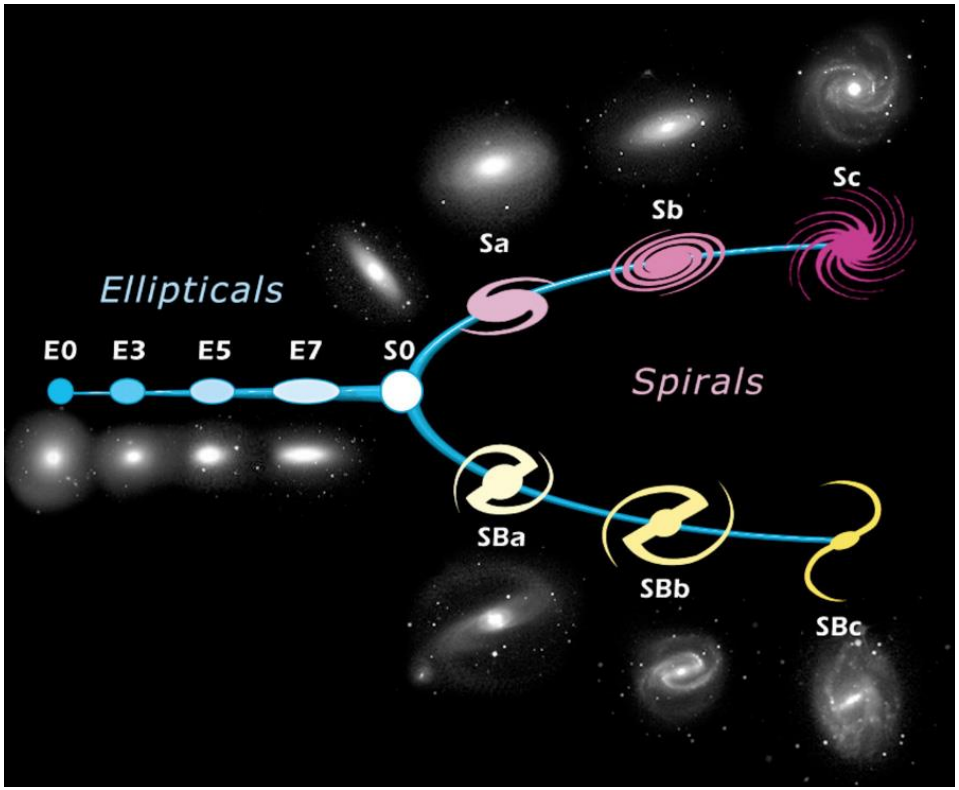

Hubble, 1926

Galaxies

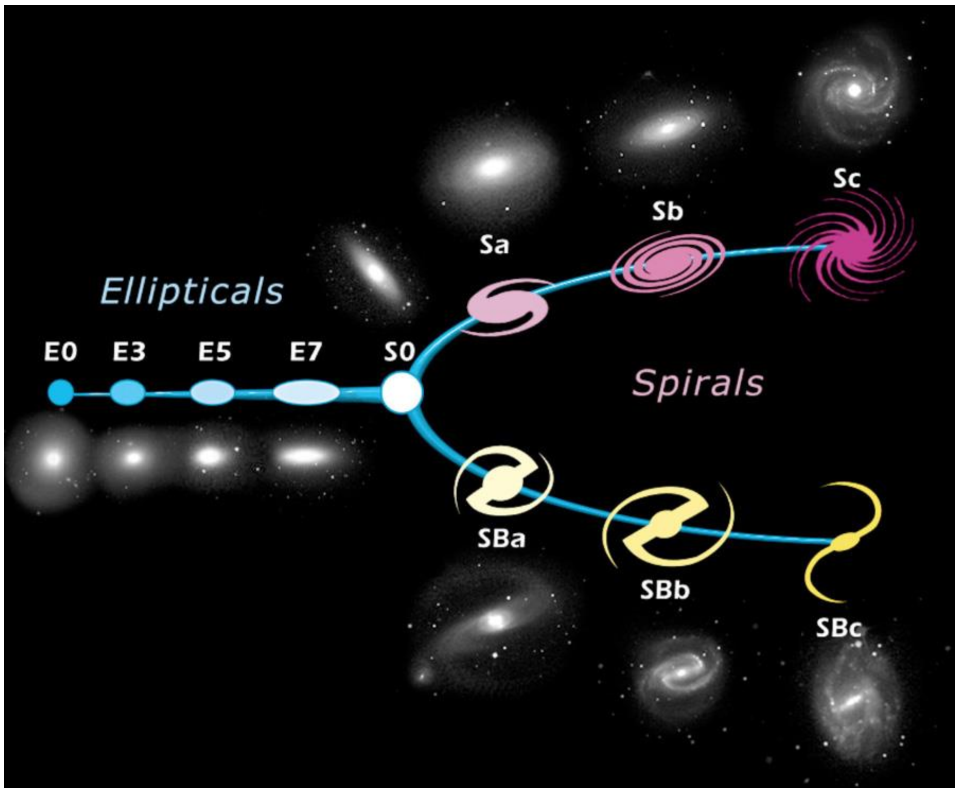

Hubble, 1926

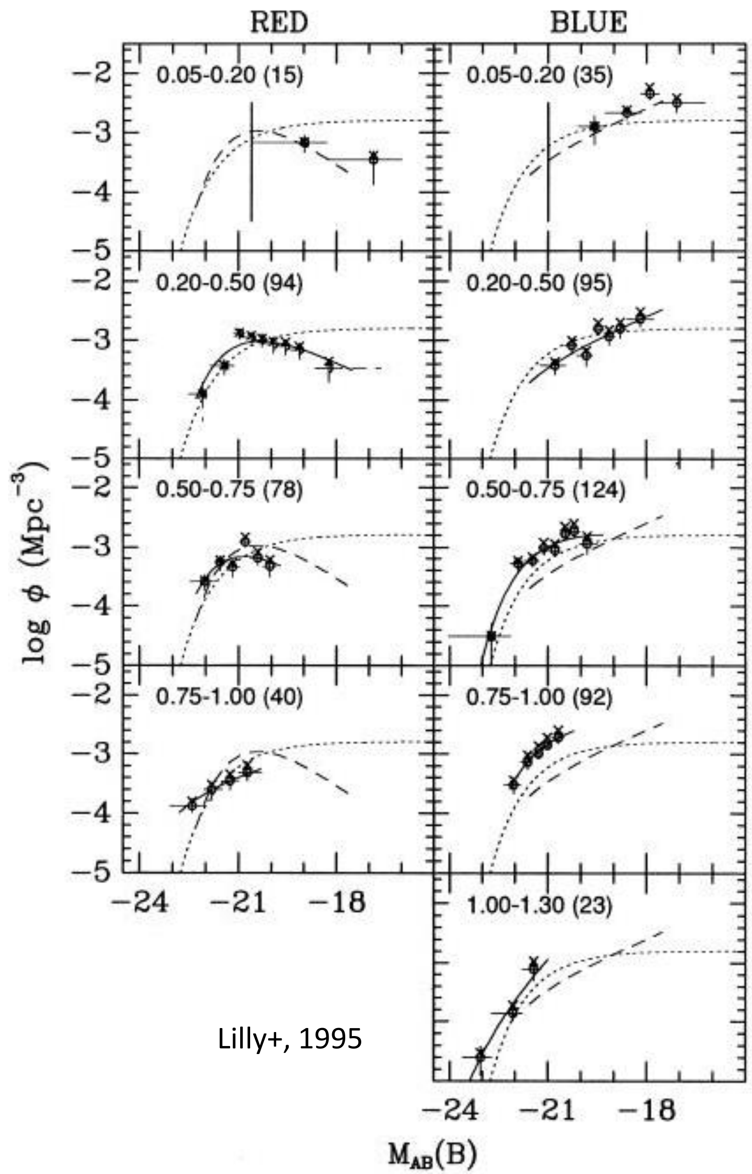

Lilly+, 1995

Study environmental dependence of galaxy properties
S. Dodonov, A. Grokhovskaya

Study environmental dependence of galaxy properties
S. Dodonov, A. Grokhovskaya

Red galaxies

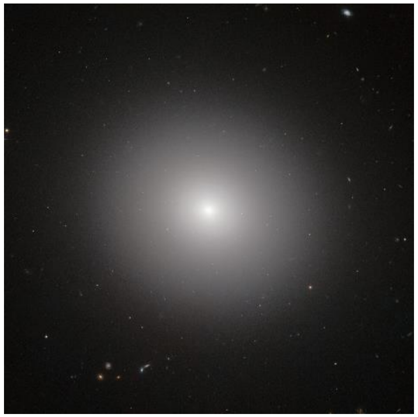

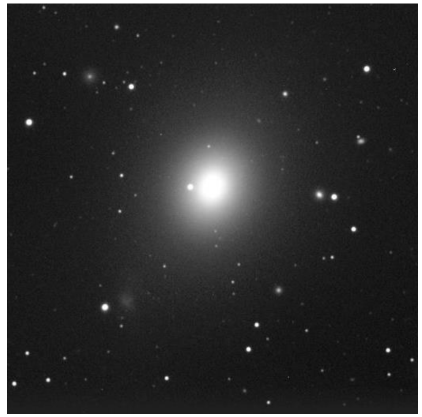

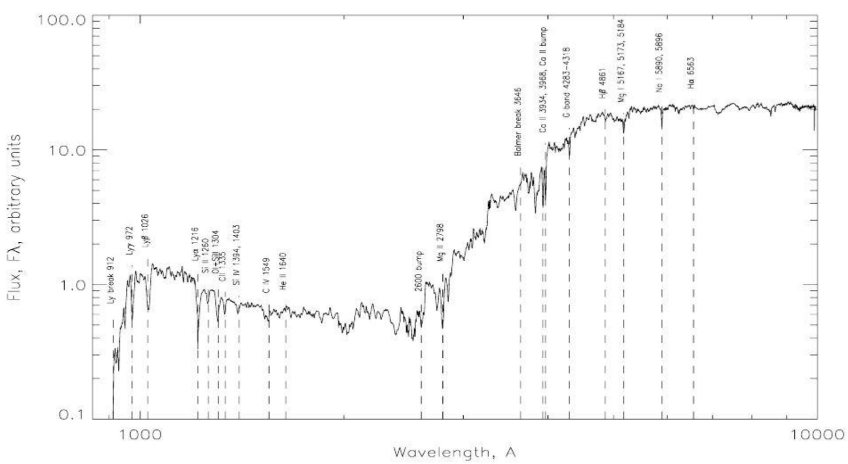

Composite spectrum of elliptical galaxy

Blue galaxies

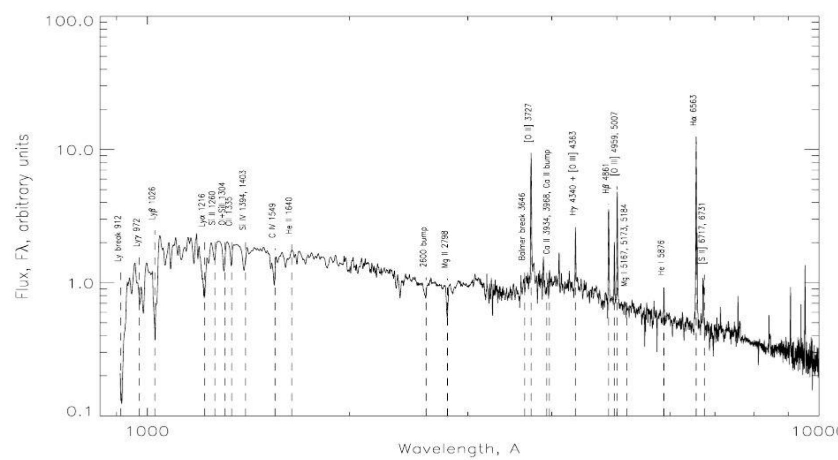

Composite spectrum of Sc/SBc/Scd/SBcd galaxy

Dodonov & Chilingarian 2008

Morphology - density relation

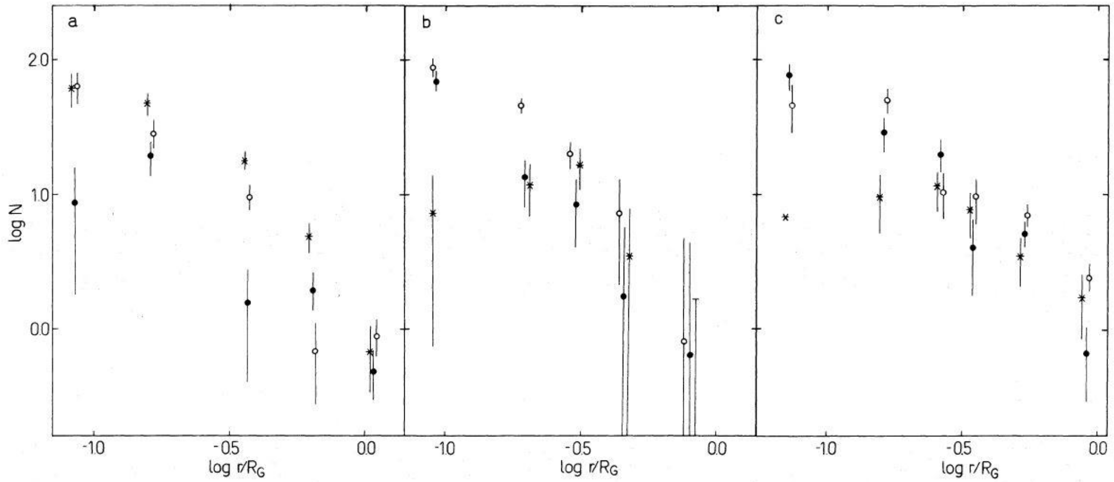

FIG. 9.—Composite projected number density profiles for spiral-rich (*a*), spiral-poor (*b*), and cD clusters (*c*). Spirals are denoted by stars; S0's, by open circles; and ellipticals, by filled circles.

Dresser, 1980

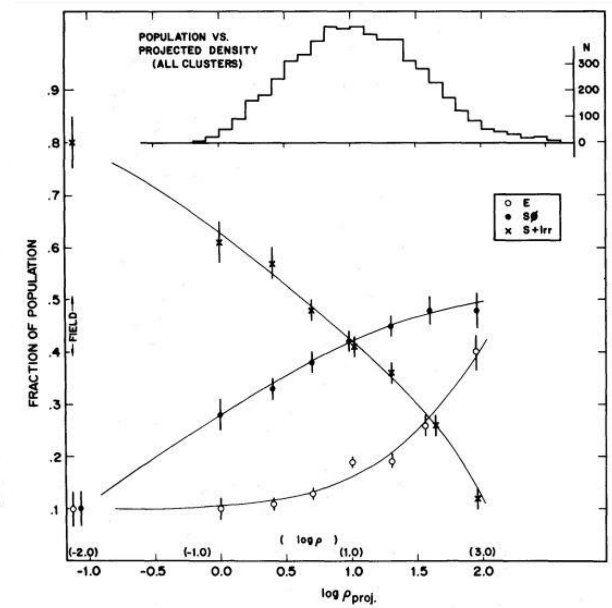

FIG. 4.—The fraction of E, S0, and S+I galaxies as a function of the log of the projected density, in galaxies Mpc^{-2}. The data shown are for all cluster galaxies in the sample and for the field. Also shown is an estimated scale of true space density in galaxies Mpc^{-3}. The upper histogram shows the number distribution of the galaxies over the bins of projected density.

Oemler, 1974

Morphology - density relation

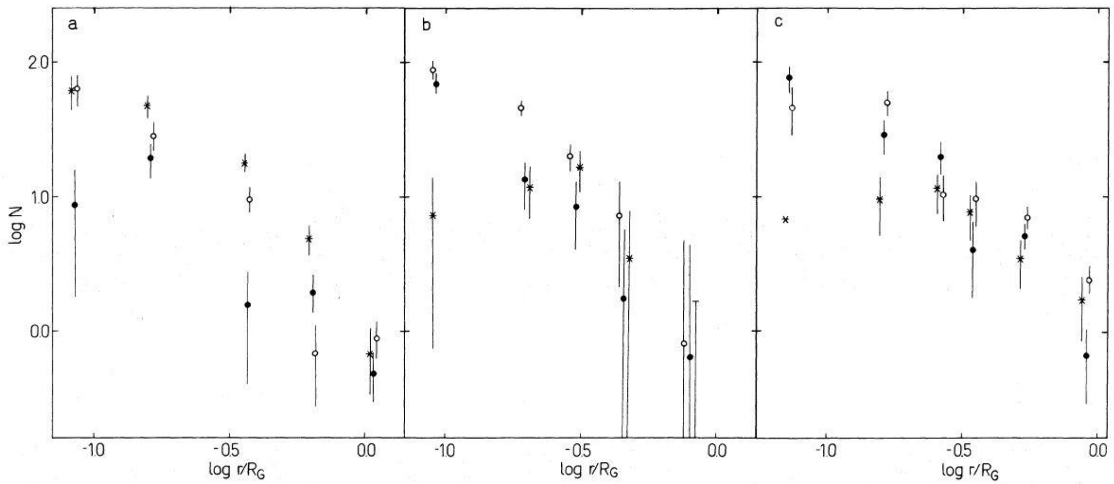

FIG. 9.—Composite projected number density profiles for spiral-rich (*a*), spiral-poor (*b*), and cD clusters (*c*). Spirals are denoted by stars; S0's, by open circles; and ellipticals, by filled circles.

Oemler, 1974

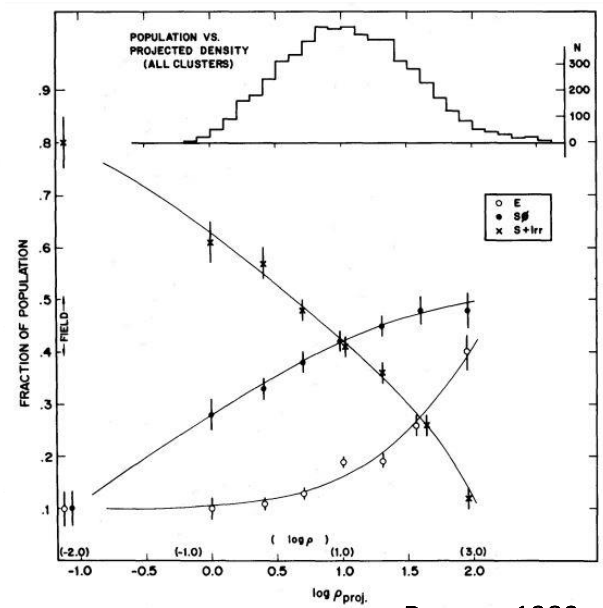

Dresser, 1980

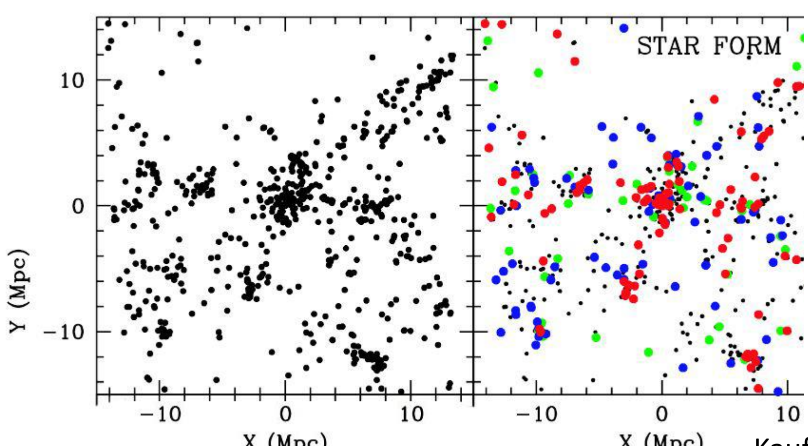

Kauffman+, 2004

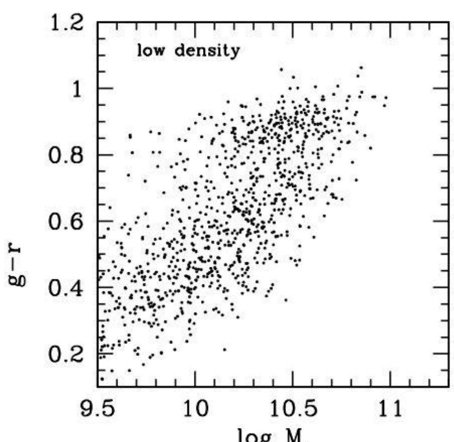

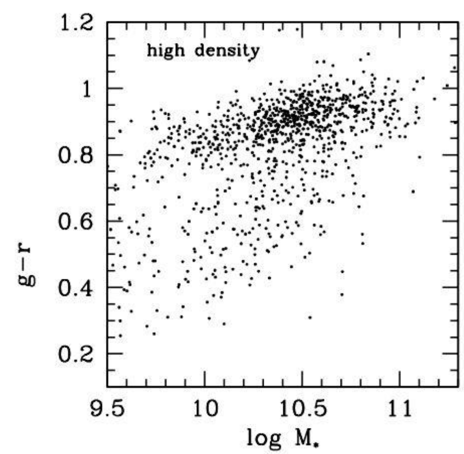

Feedback

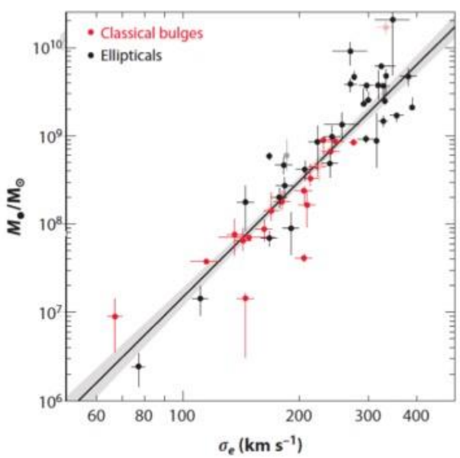

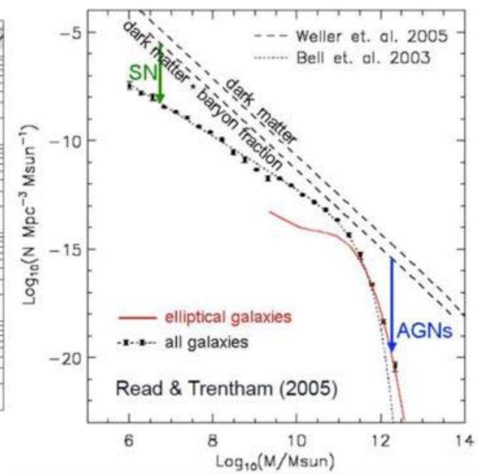

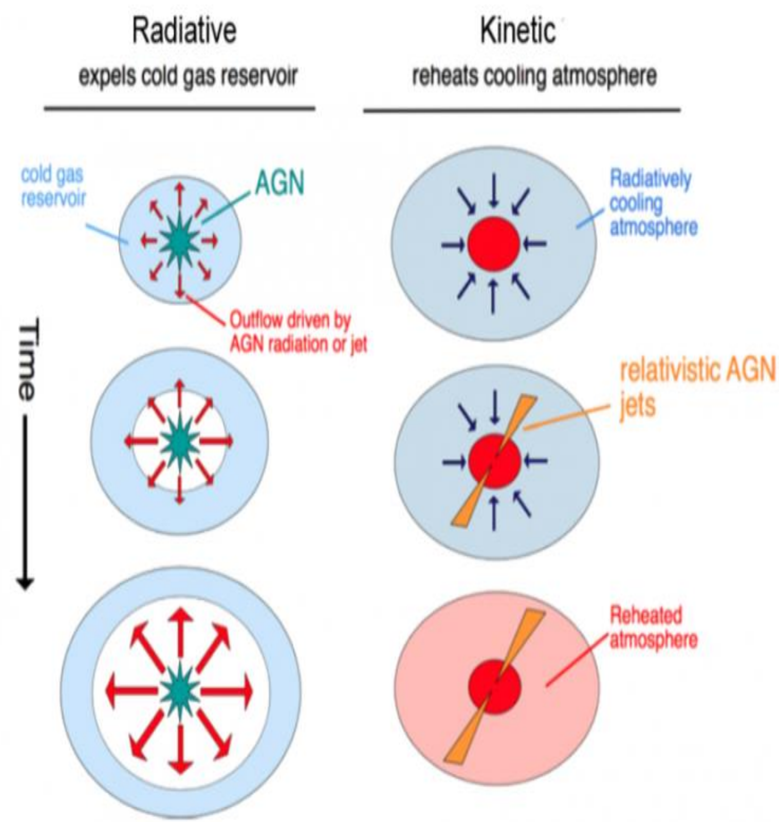

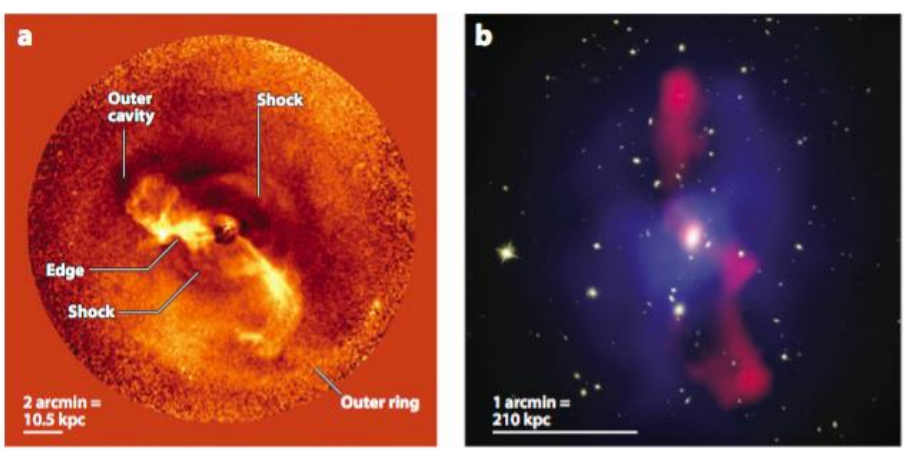

Fabian +, 2012

How AGNs can acts on physical parameters in galaxy clusters?

The observations

Observations on 1-m Schmidt Telescope

Telescope field of view with 4k x 4k CCD 58 x 58 arcmin, scale 0.868 arcsec/pixel. Observations were in four broad band filters (u, g, r and i SDSS) and in 15 medium band (FWHM=250 A) filters. Total exposure time in filters were varied from 60 min to 120 min depending from the spectral sensitivity of the CCD.

Filter	λ_{cen}, A	FWHM (A)	$m_{lim,5\sigma}$
u_SDSS	3578	338	24.23
g_SDSS	4797	860	25.22
r_SDSS	6227	770	24.97
i_SDSS	7624	857	24.15
MB_400	3978	250	24.37
MB_425	4246	250	24.31
MB_450	4492	250	24.20
MB_475	4745	250	24.31
MB_500	4978	250	24.30
MB_525	5234	250	24.37
MB_550	5496	250	23.86
MB_575	5746	250	24.29
MB_600	5959	250	23.89
MB_625	6234	250	23.51
MB_650	6499	250	23.41
MB_675	6745	250	23.78
MB_700	7002	250	23.47
MB_725	7253	250	23.20
MB_750	7519	250	23.07
MB_775	7758	250	22.97

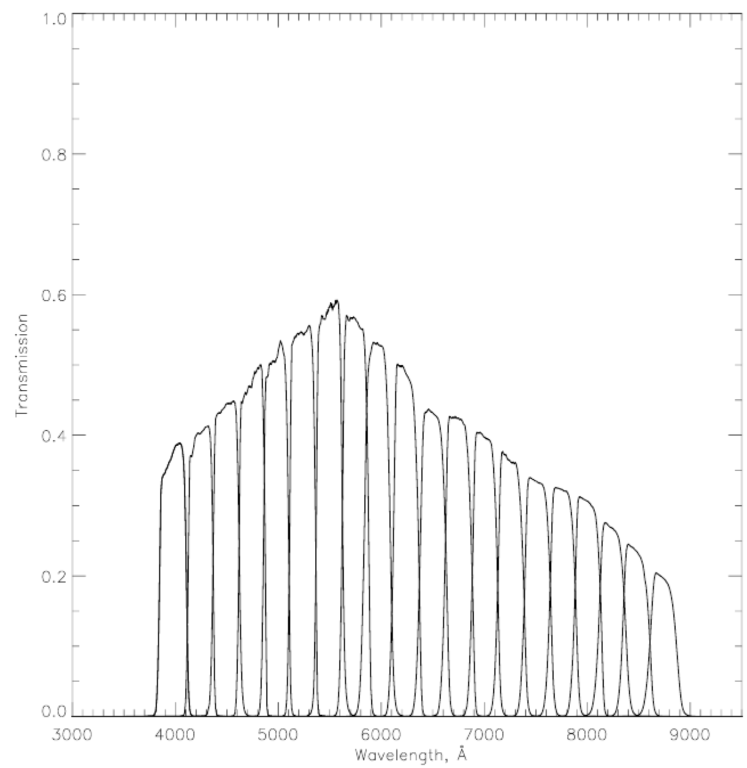

Medium band filters set used in observations. CCD spectral response included.

ROSAT survey in the HQS field HS47.5-22

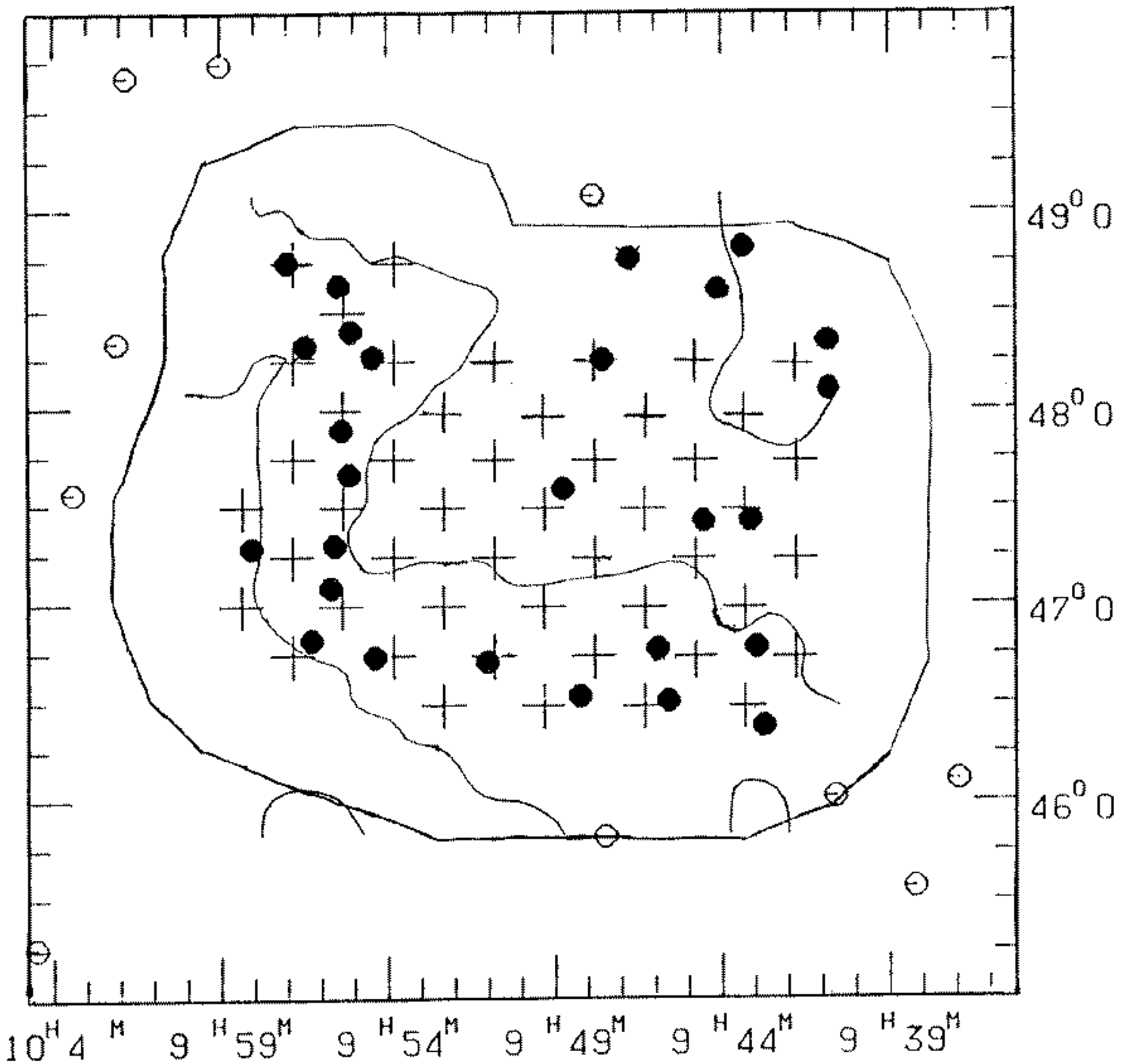

48 overlapping PSPC pointings

574 X-ray sources

K. Molthagen+, 1997

Galaxies sample definition

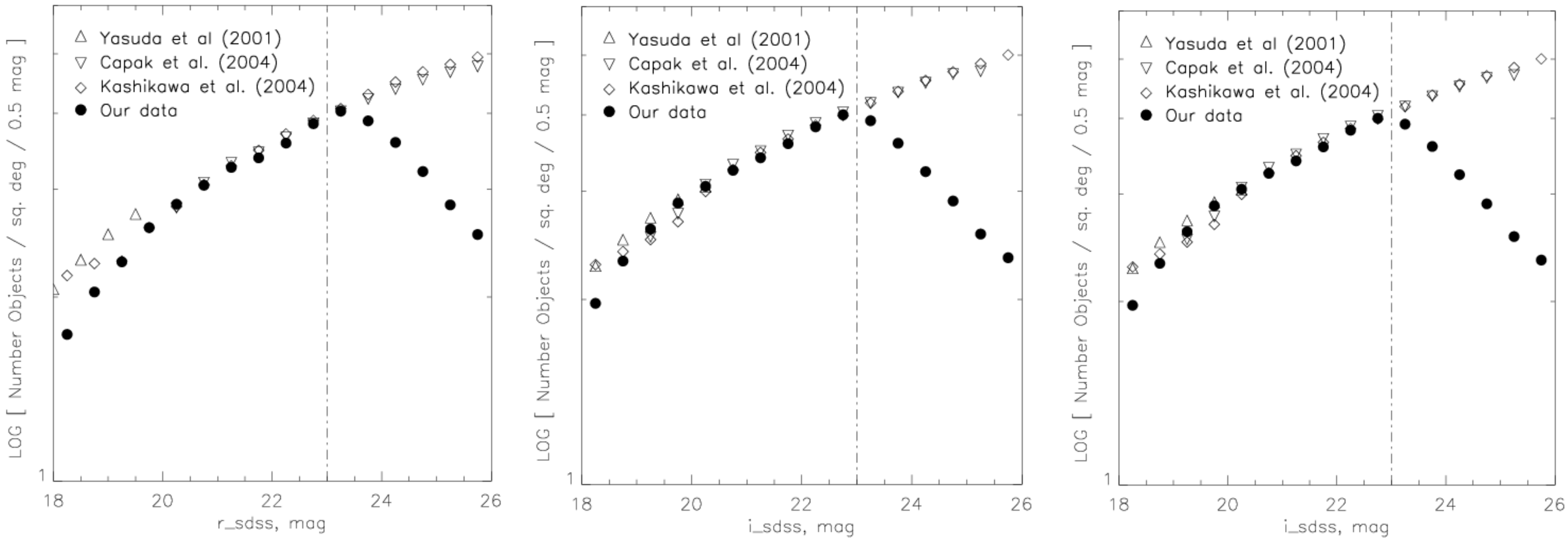

Galaxies sample is extracted from the full catalog of objects (near 100000 objects) using following criteria :

- Objects brighter then RAB=23m ;
- Extended index < 0.8;
- Index of contamination ≤ 2.

Into the final sample follow first two criteria we include 39669 objects and after applying third one - we have 36447 objects with clean photometry. Due to the contamination we lose 8.12 % of the objects.

We check sample completeness using comparison of galaxies number-counts in g, r and i SDSS filters from our sample with already published data.

HS47.5-22

RA = $09^h50^m00^s$
DEC = $+47^d35^m00^s$

Field 2.39 sq. deg.

36447 Galaxies
to $R_{AB}=23^m$ with
clean photometry

574 ROSAT Objects
to $3.5*10^{-14}$ ergs
$cm^{-2}s^{-1}$

362 FIRST Objects

293 SDSS QSO

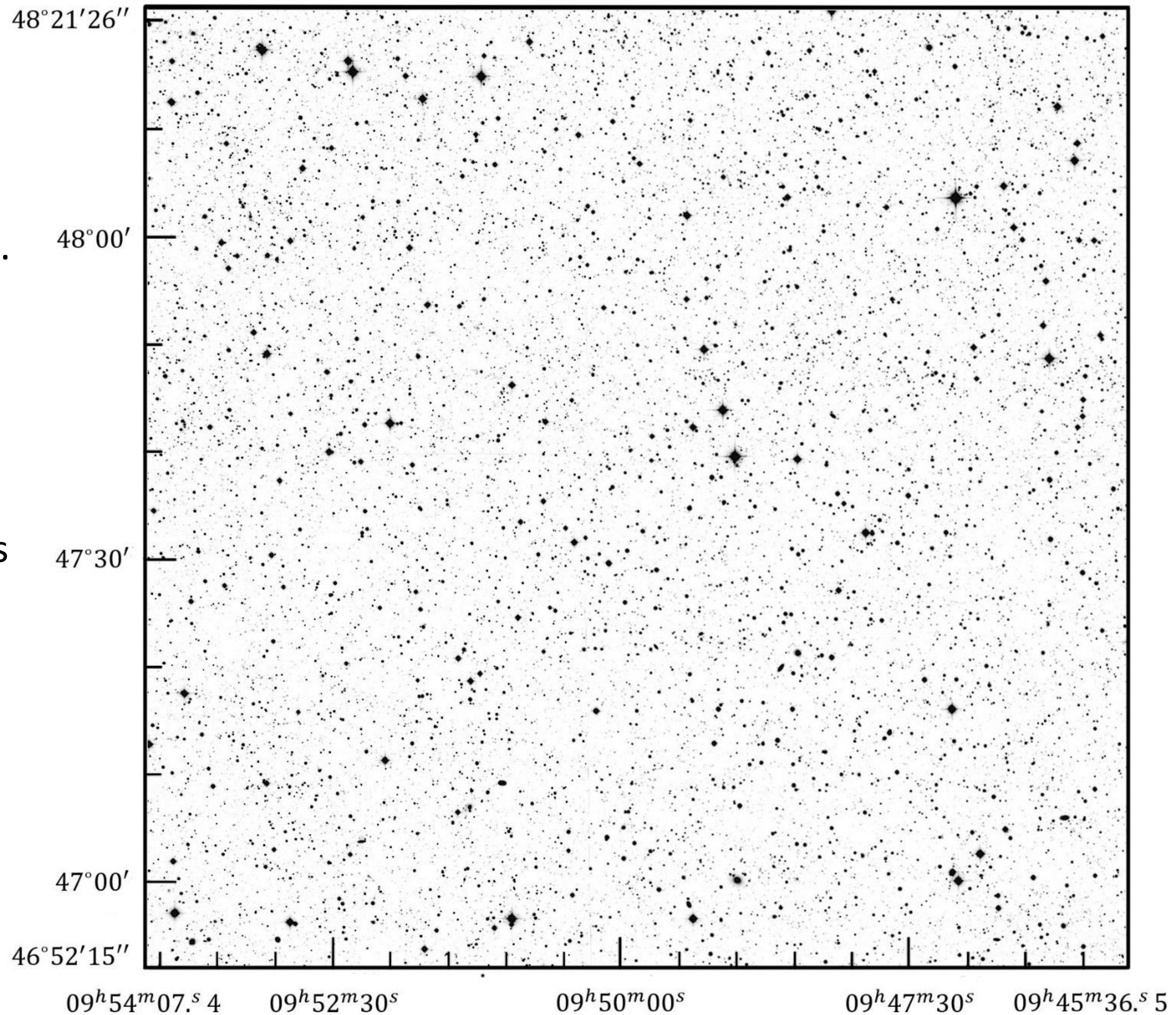

SEDs Analysis

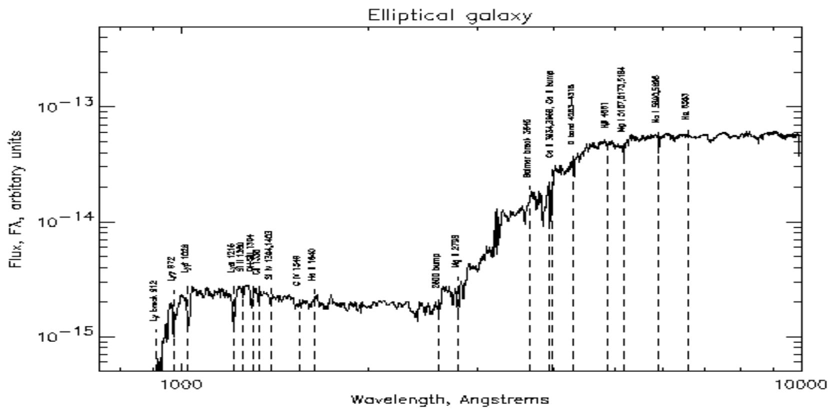

The photometric measurements from filters set provide low resolution spectra for each object which are analyzed by a statistical technique for classification and redshift estimation based on spectral template matching.

For SEDs analysis should be used :

- Stellar spectra library;
- Galaxies spectra library;
- QSO's spectra library.

Priors for a galaxy with given magnitude having redshift Z.

Star – Galaxy morphology classification index.

As a result we get a probability that object with given SED classified as galaxy or QSO, or Star with known spectral type and redshift.

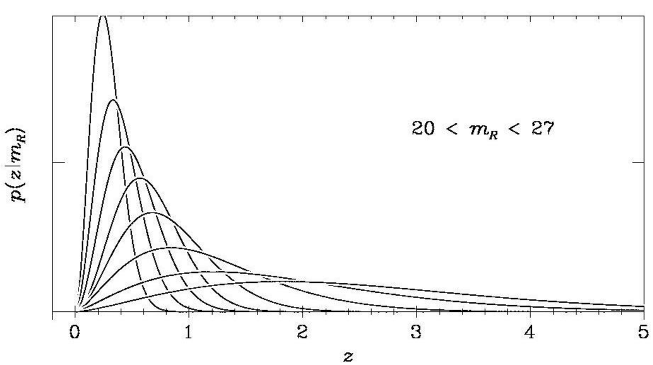

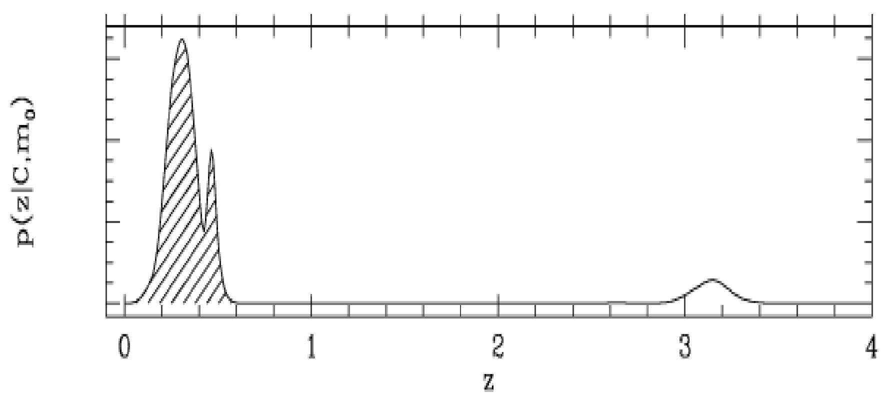

SEDs Analysis

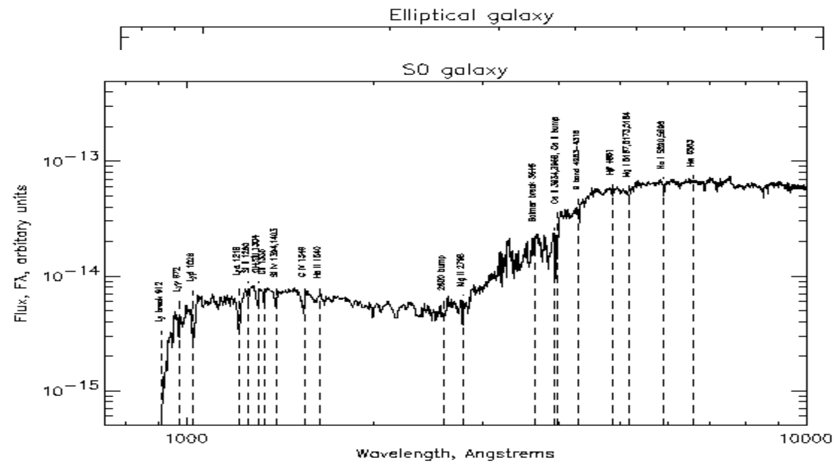

The photometric measurements from filters set provide low resolution spectra for each object which are analyzed by a statistical technique for classification and redshift estimation based on spectral template matching.

For SEDs analysis should be used :

- Stellar spectra library;
- Galaxies spectra library;
- QSO's spectra library.

Priors for a galaxy with given magnitude having redshift Z.

Star – Galaxy morphology classification index.

As a result we get a probability that object with given SED classified as galaxy or QSO, or Star with known spectral type and redshift.

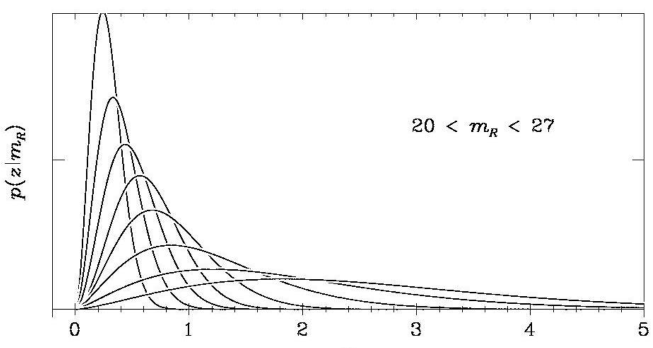

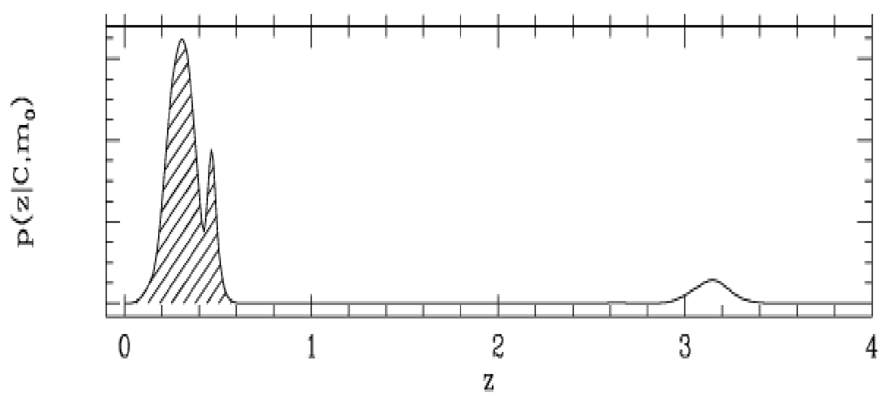

SEDs Analysis

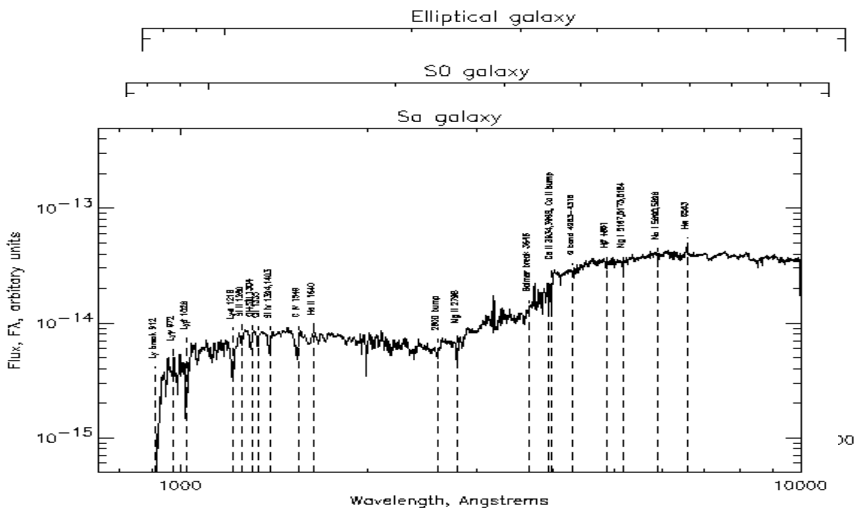

The photometric measurements from filters set provide low resolution spectra for each object which are analyzed by a statistical technique for classification and redshift estimation based on spectral template matching.

For SEDs analysis should be used :

- Stellar spectra library;
- Galaxies spectra library;
- QSO's spectra library.

Priors for a galaxy with given magnitude having redshift Z.

Star – Galaxy morphology classification index.

As a result we get a probability that object with given SED classified as galaxy or QSO, or Star with known spectral type and redshift.

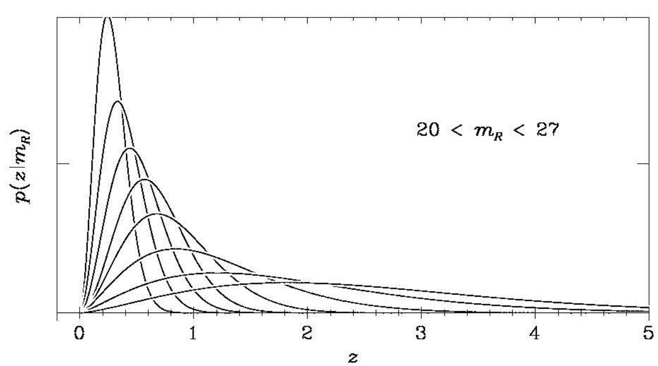

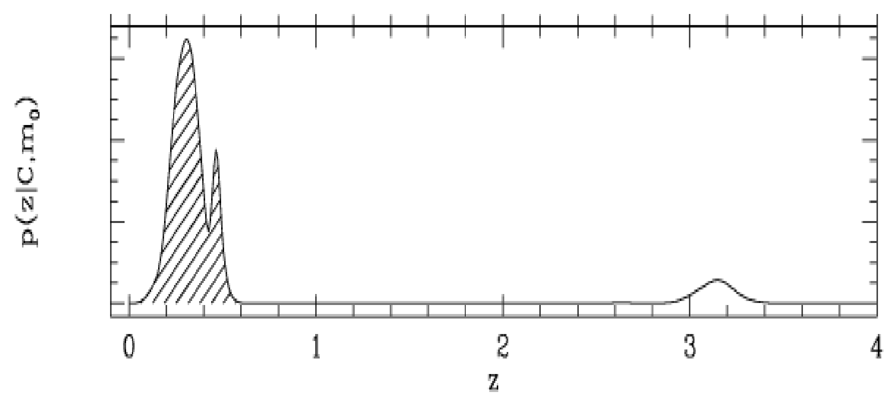

SEDs Analysis

The photometric measurements from filters set provide low resolution spectra for each object which are analyzed by a statistical technique for classification and redshift estimation based on spectral template matching.

For SEDs analysis should be used :

- Stellar spectra library;
- Galaxies spectra library;
- QSO's spectra library.

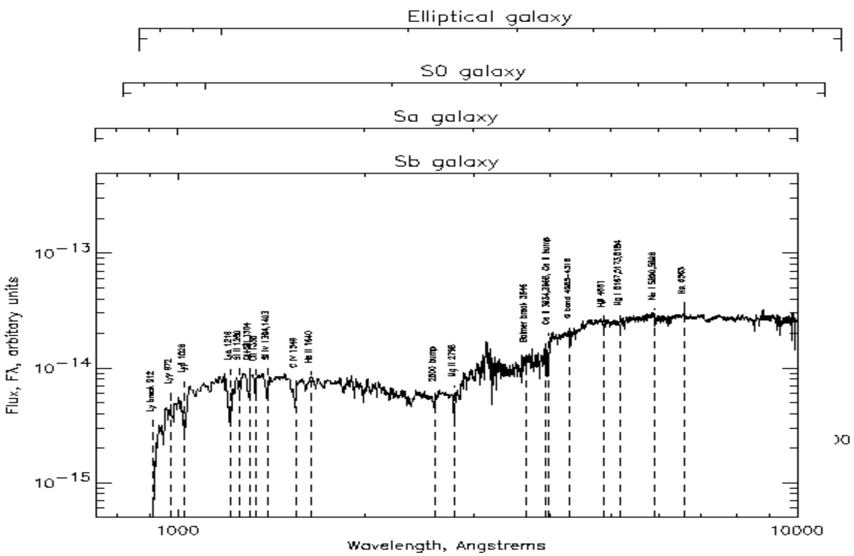

Priors for a galaxy with given magnitude having redshift Z.

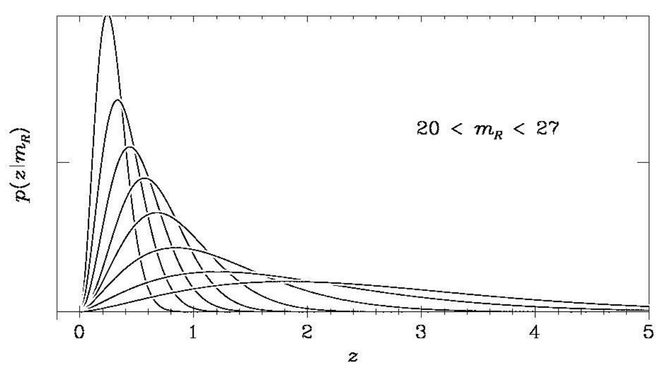

Star – Galaxy morphology classification index.

As a result we get a probability that object with given SED classified as galaxy or QSO, or Star with known spectral type and redshift.

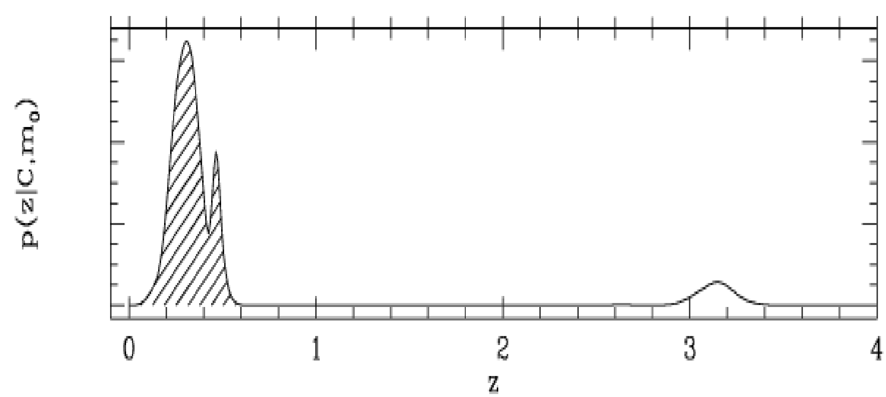

SEDs Analysis

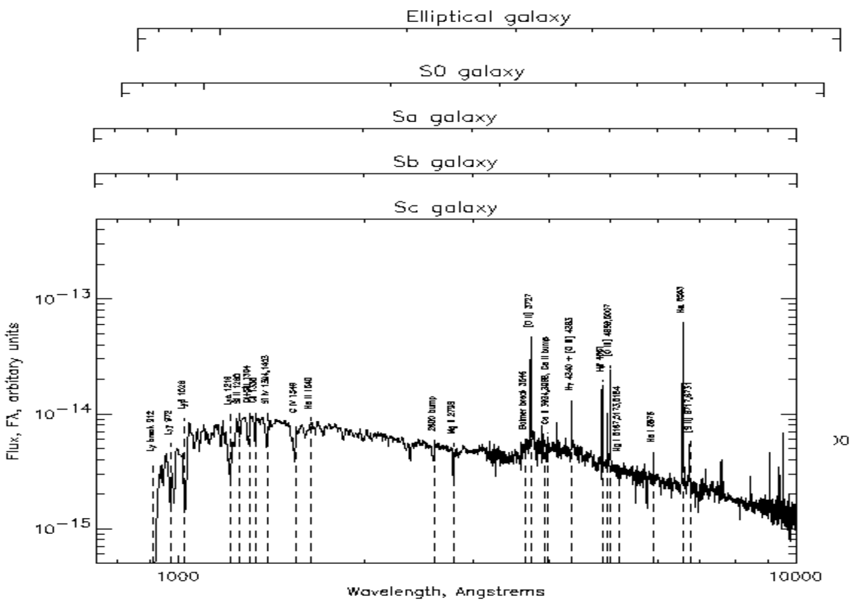

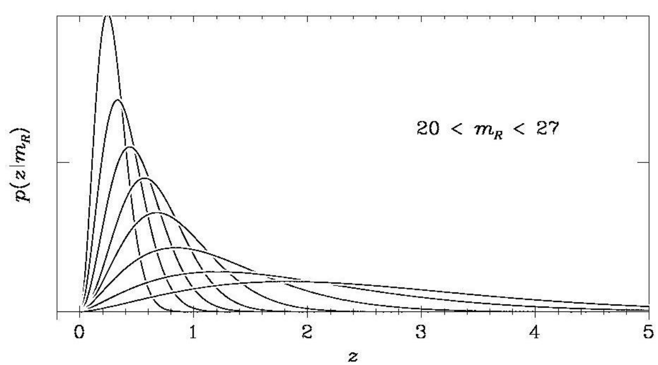

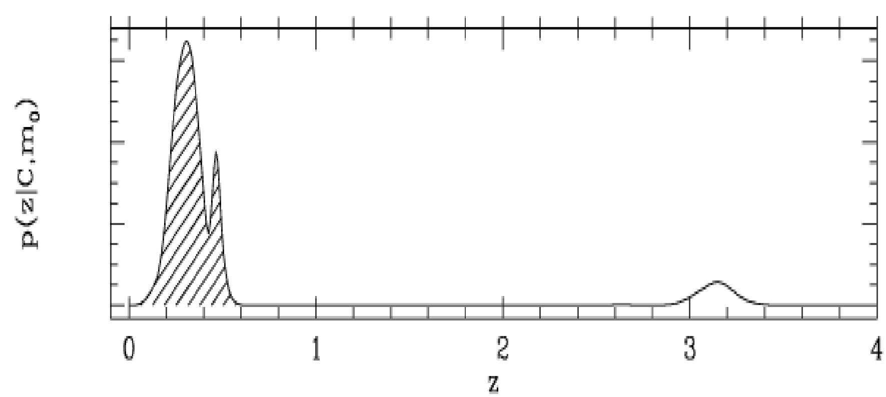

The photometric measurements from filters set provide low resolution spectra for each object which are analyzed by a statistical technique for classification and redshift estimation based on spectral template matching.

For SEDs analysis should be used :

- Stellar spectra library;
- Galaxies spectra library;
- QSO's spectra library.

Priors for a galaxy with given magnitude having redshift Z.

Star – Galaxy morphology classification index.

As a result we get a probability that object with given SED classified as galaxy or QSO, or Star with known spectral type and redshift.

SEDs Analysis

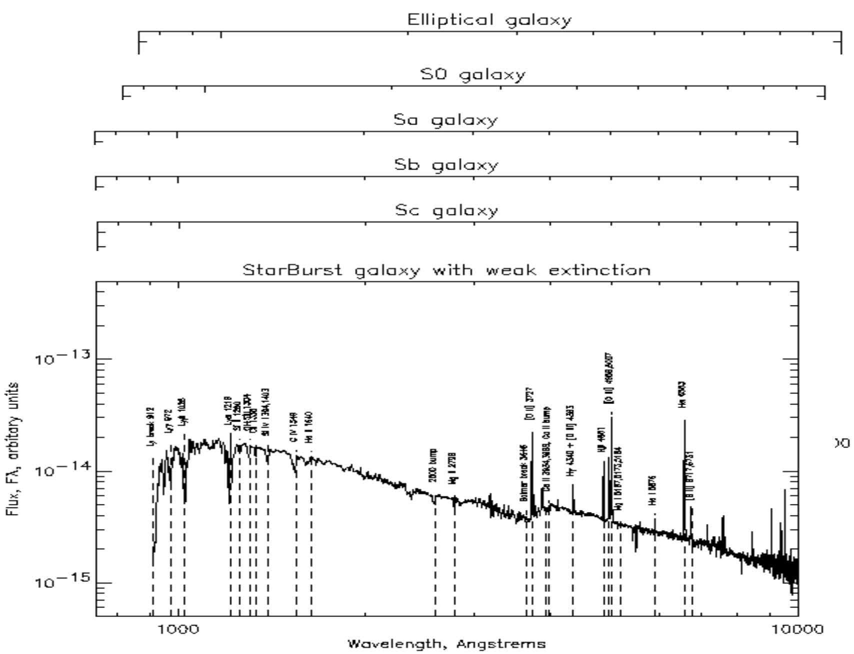

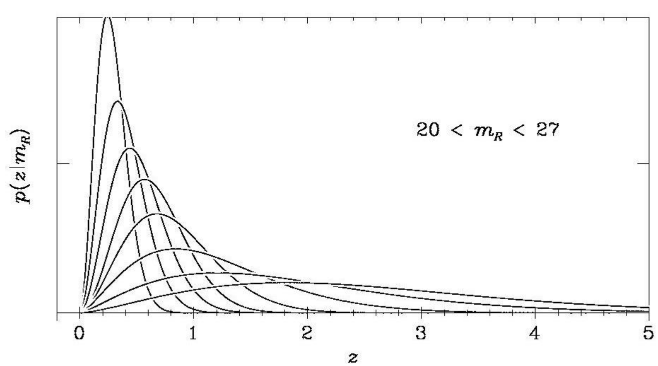

The photometric measurements from filters set provide low resolution spectra for each object which are analyzed by a statistical technique for classification and redshift estimation based on spectral template matching.

For SEDs analysis should be used :

- Stellar spectra library;
- Galaxies spectra library;
- QSO's spectra library.

Priors for a galaxy with given magnitude having redshift Z.

Star – Galaxy morphology classification index.

As a result we get a probability that object with given SED classified as galaxy or QSO, or Star with known spectral type and redshift.

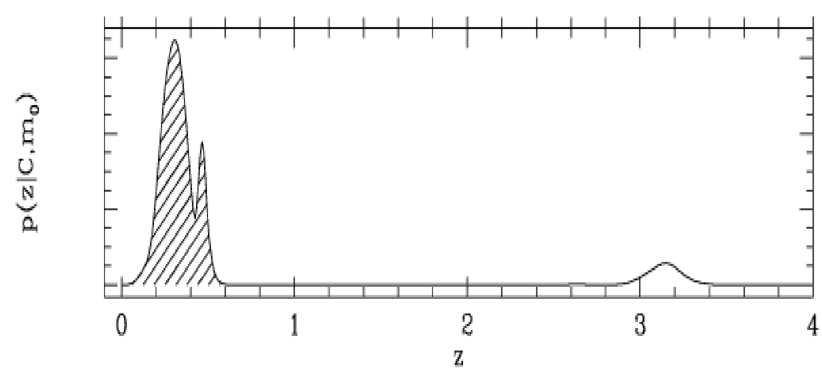

Spectral Energy Distribution vs SDSS Spectra

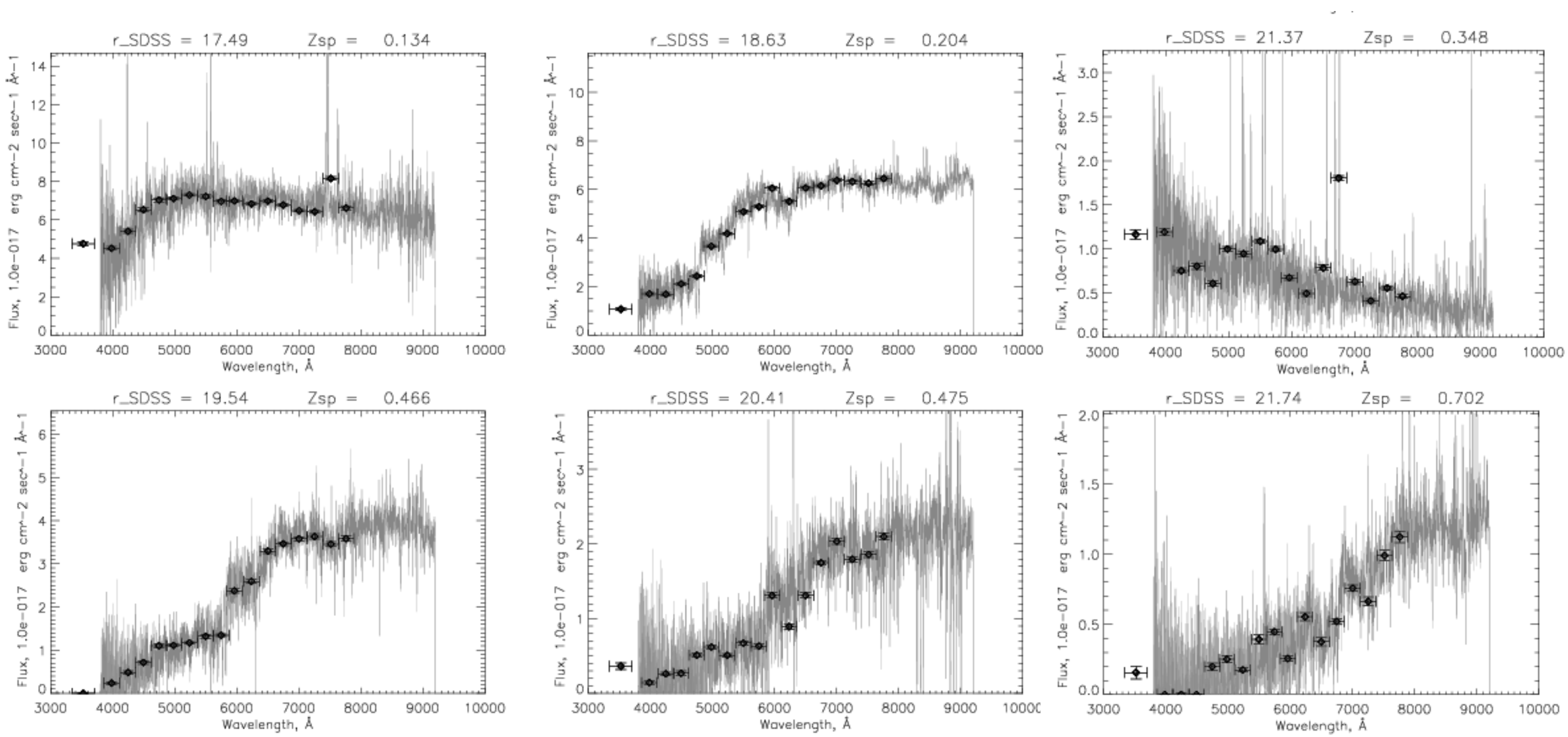

Photometric redshifts

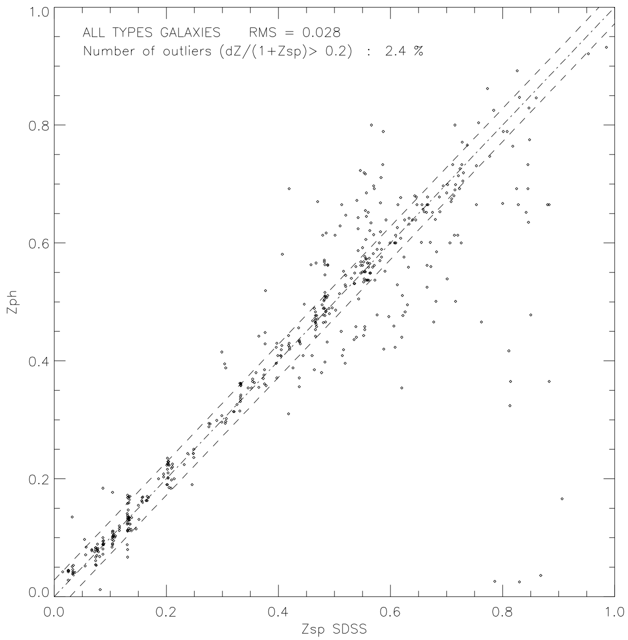

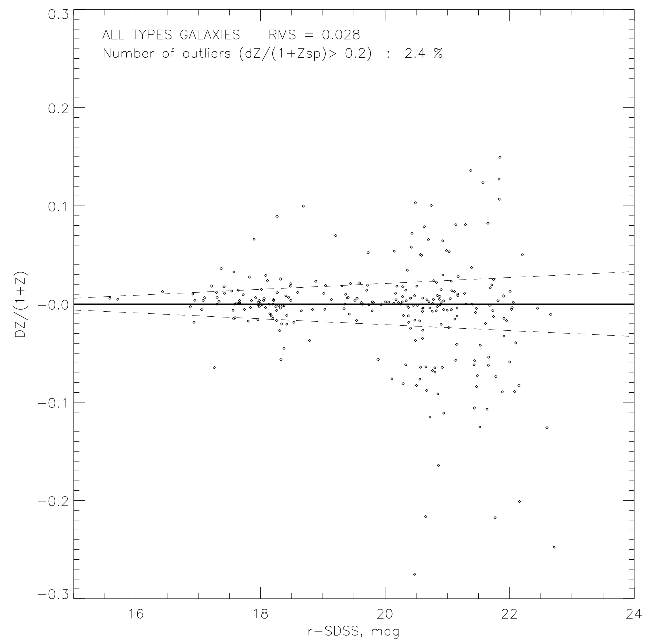

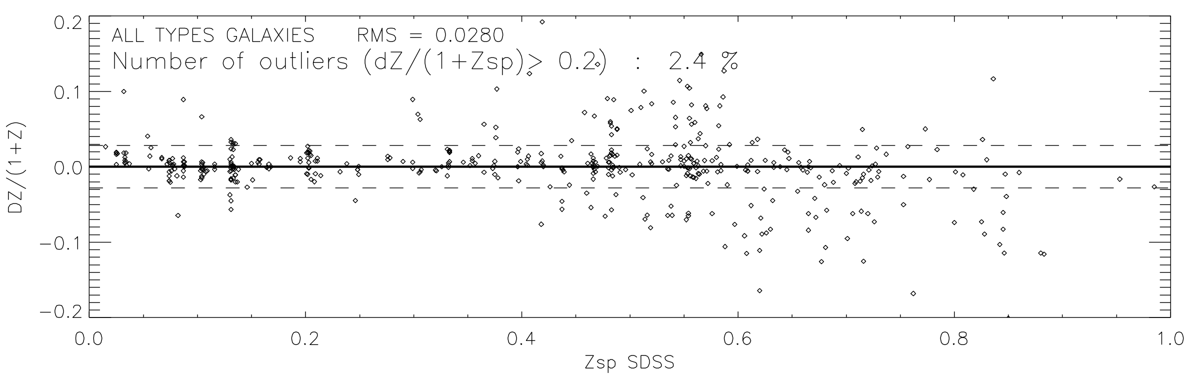

Comparison between photometric redshifts Zph obtained with ZEBRA in Maximum Likelihood mode with SDSS spectroscopic redshifts Zsp along with error distribution $\Delta Z/(1+Z)$ for all galaxies with known spectroscopic redshifts.

Obtained accuracy σz < 0.028 and fraction of catastrophic outliers ($\Delta Z/(1+Z) > 0.2$) ~ 2.4%. Accuracy σz changes from 0.011 in magnitude range r_SDSS =16m – 20m till 0.066 in magnitude range r_SDSS = 21m – 23m.

HS 47.5 + 22 is deep wide homogeneous field (2.386 sq. deg.) with determined x-ray and radio sources in the field
There is only one more the same field (COSMOS field)

The data analysis

Group and clusters of galaxies. First catalogs

THE DISTRIBUTION OF RICH CLUSTERS OF GALAXIES*

GORGE O. ABELL†
Mount Wilson and Palomar Observatories
Carnegie Institution of Washington, California Institute of Technology
Received September 30, 1957; revised November 13, 1957

ABSTRACT

A catalogue is prepared of 2712 rich clusters of galaxies found on the National Geographic Society–Palomar Observatory Sky Survey. From the catalogue, 1682 clusters are selected which meet specific criteria for inclusion in a homogeneous statistical sample. An investigation of the sample leads to the following conclusions: (1) the distribution function
rapidly as *n* decreases; (2) the data allow no significan
varies with distance; (3) galactic obscuration of the or
at high northern galactic latitudes around galactic lo
random surface distribution of clusters, both when cl
distances are considered. An analysis of the distribut
second-order clusters, that is, clusters of clusters of gal
between the observed distribution and one of comple

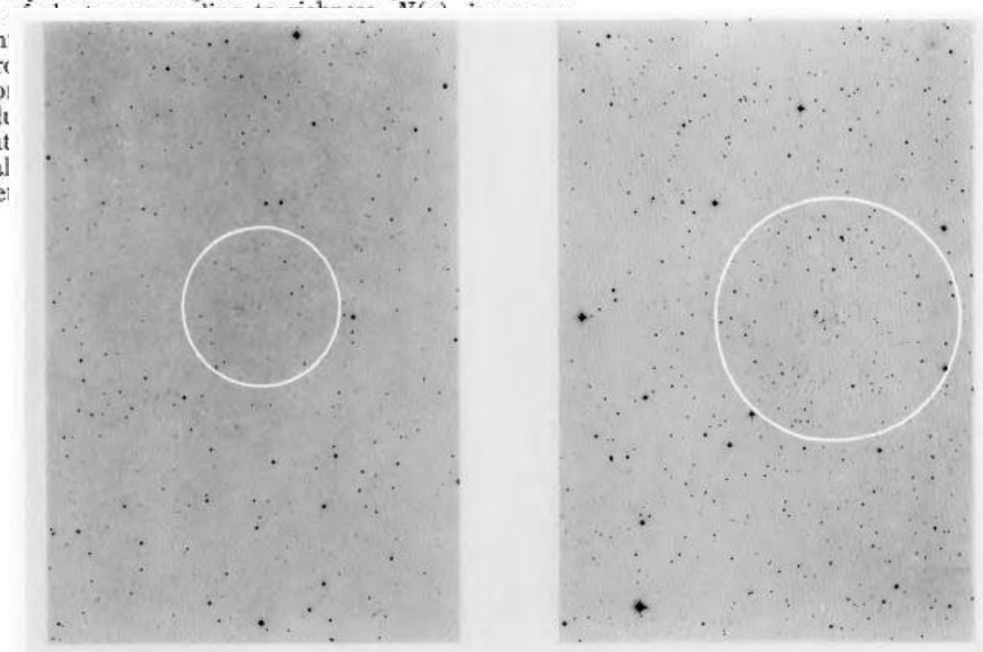

Group and clusters of galaxies. First catalogs

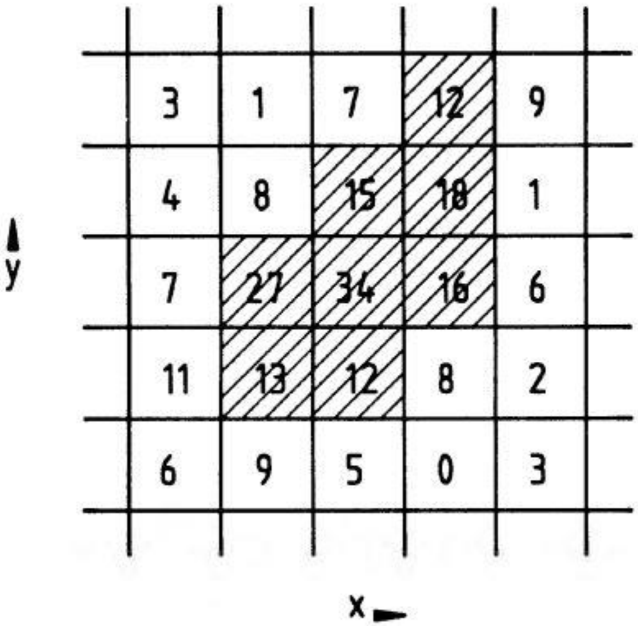

FIG. 1. Subset of galaxy counts from COSMOS scans of a photographic plate with the count resolution being 5′×5′.

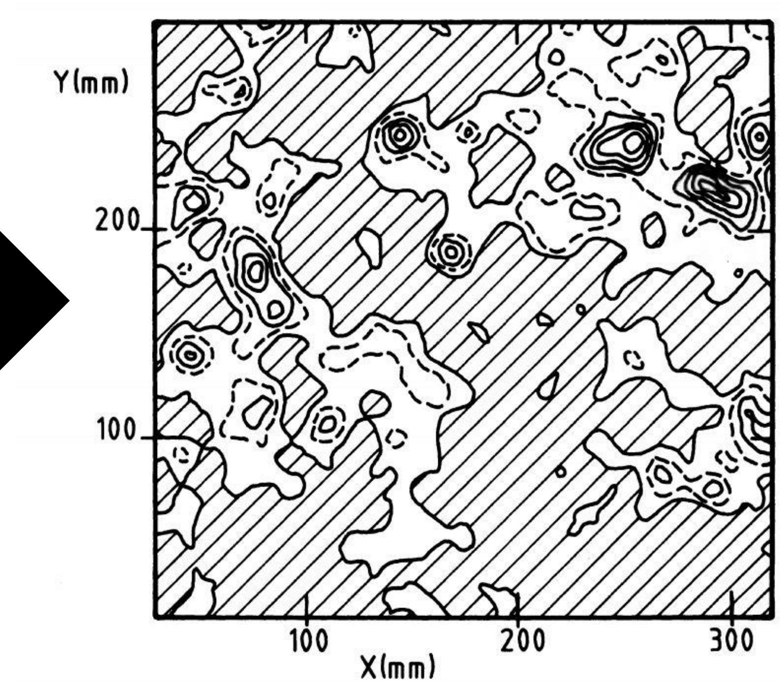

FIG. 2. Distribution of galaxies detected down to $B=21.5$ in field 411 of the ESO/SERC Southern Sky survey. Hatched areas represent areas of the data in which the galaxy numbers are below the overall mean level of 8 (from counts in 5′×5′). The first isoplethal level is at the mean level, and subsequent isopleths are at intervals of three galaxies per cell thereafter.

Shectman+, 1985; Dodd, MacGillivray, 1986

Methods

1. X-ray emission from hot gas

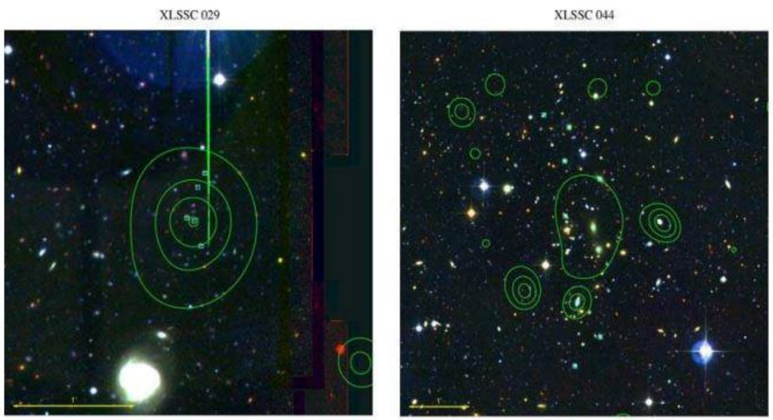

M. Pierre +, 2006

Methods

1. X-ray emission from hot gas

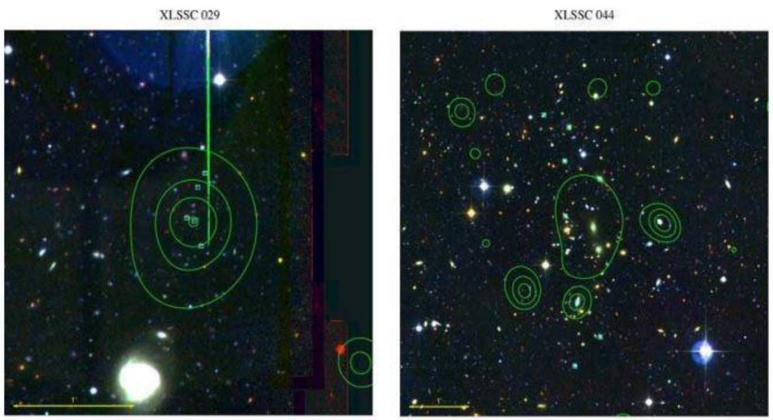

M. Pierre +, 2006

2. Sunyaev–Zel'dovich effect in the CMB

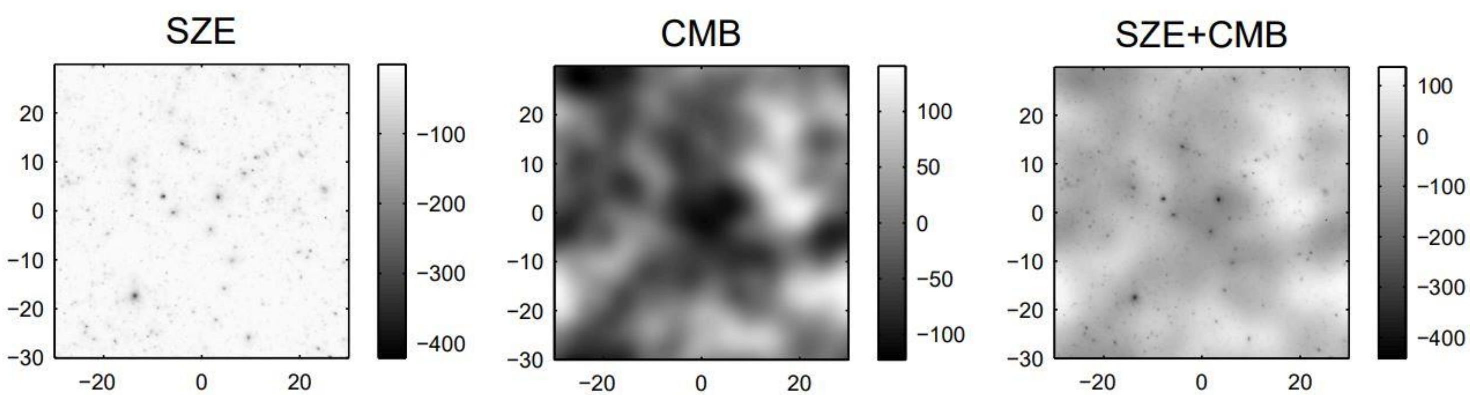

Carlstrom +, 2002

Methods

3. Cosmic shear due to weak gravitational lensing

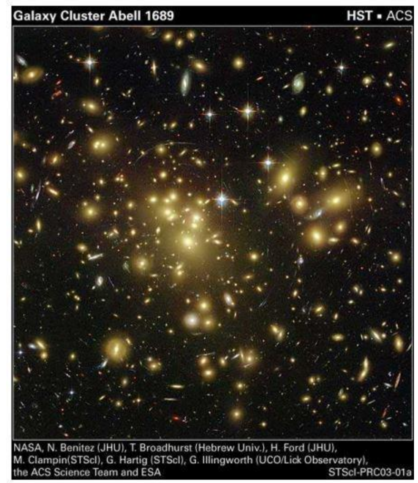

1. X-ray emission from hot gas

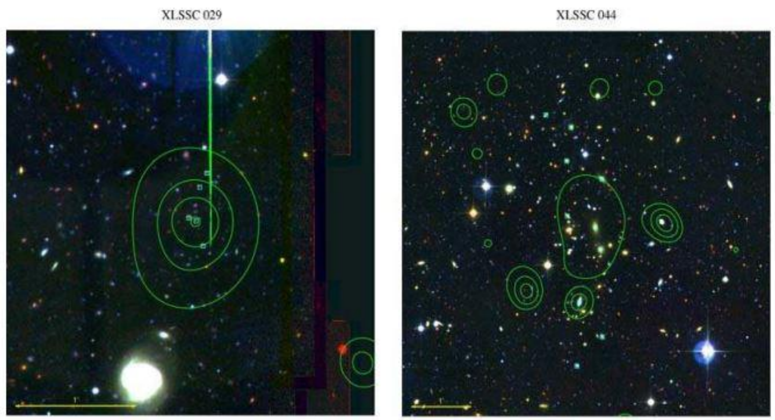

M. Pierre +, 2006

2. Sunyaev–Zel'dovich effect in the CMB

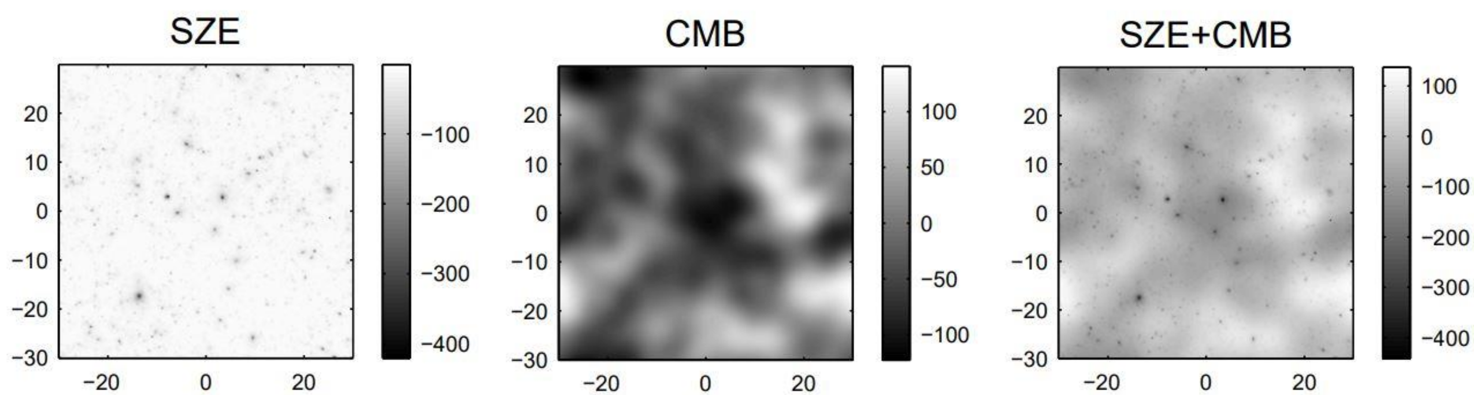

Carlstrom +, 2002

Methods

1. X-ray emission from hot gas

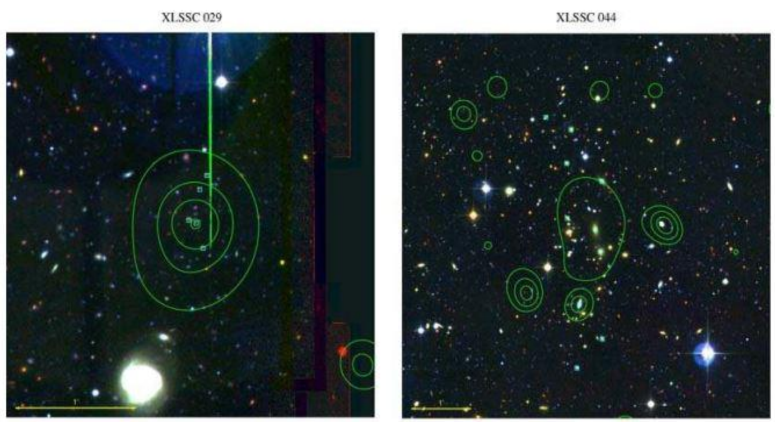

M. Pierre +, 2006

3. Cosmic shear due to weak gravitational lensing

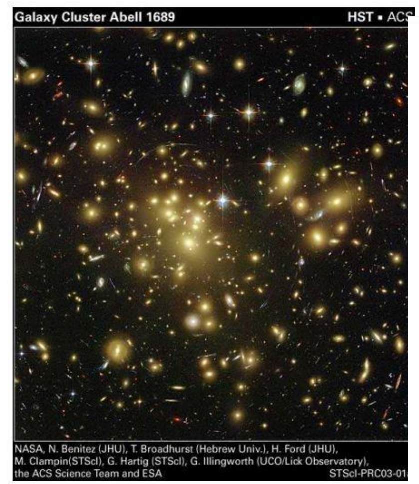

4. Galaxy overdensities in optical, near-infrared or mid-IR images

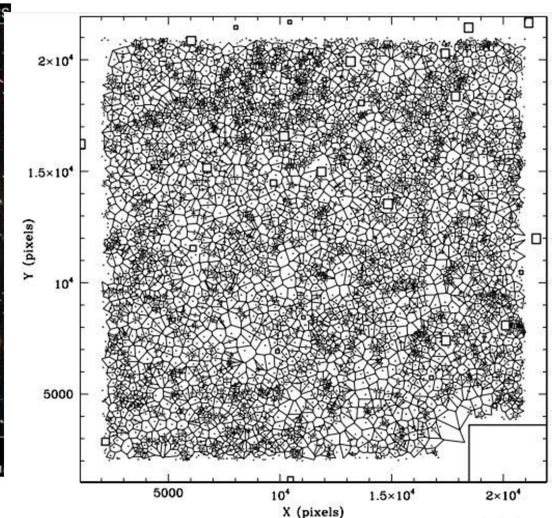

Lopes+, 2004

2. Sunyaev–Zel'dovich effect in the CMB

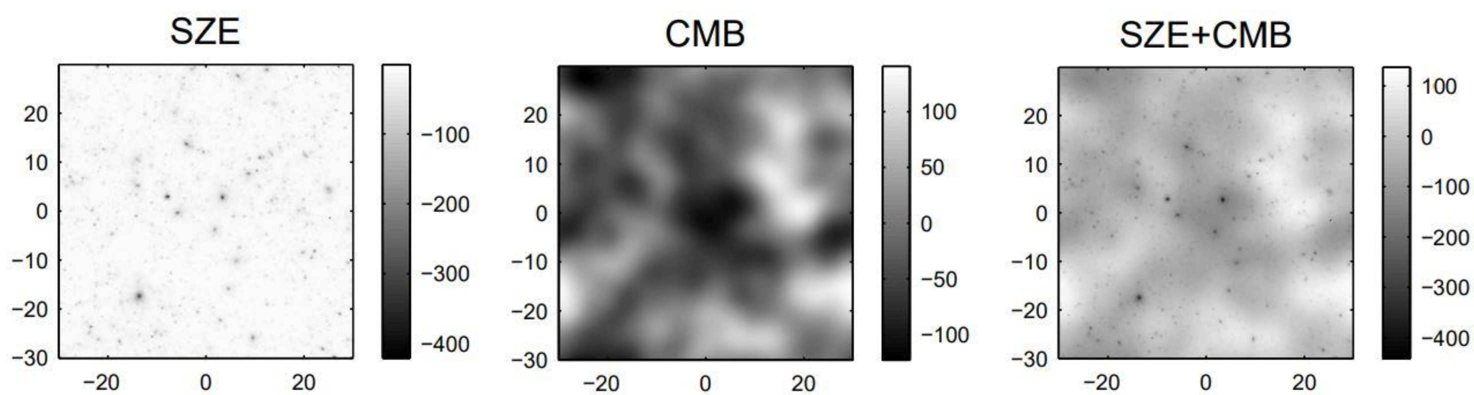

Carlstrom +, 2002

Algorithms (short, incomplete, subjective sample)

1. Counting objects projected onto the field (Shectman +, 1985; Dodd, MacGillivray, 1986)

2. Comparing the distribution functions of objects with Poisson distribution (Limber+, 1953; Neyman & Scott, 1955)

3. Cluster analysis:
   - Minimal spinning tree (Barrow, 1985)
   - Friend-of-friends (More+, 2011)
   - Comparison of correlation functions (Maller+, 2005)

4. Filtering algorithms (Kovac+, 2009)

5. Voronoi diagrams (Ramela+, 2001)

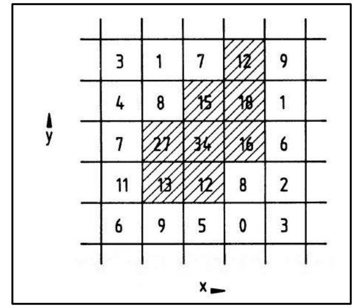

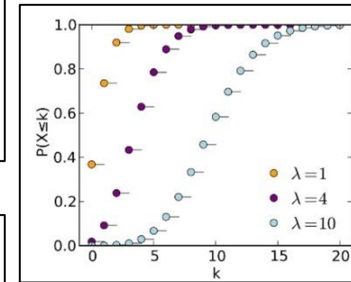

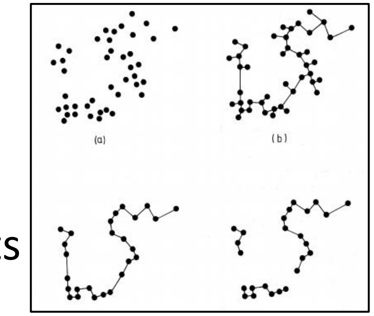

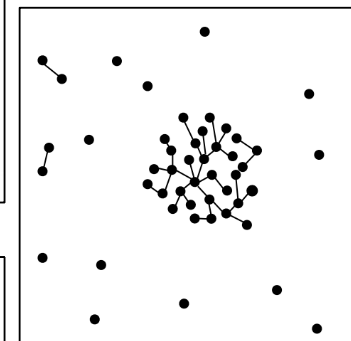

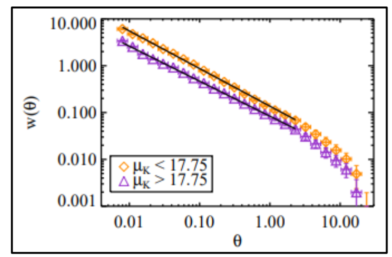

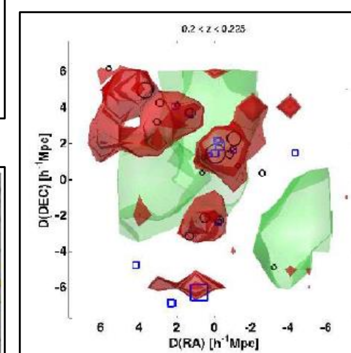

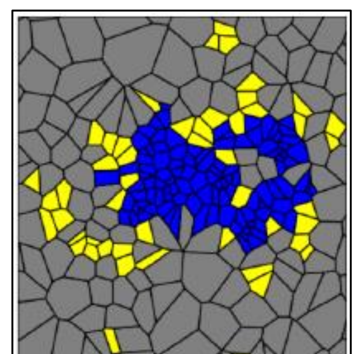

Mock catalogs

MICECAT v2 galaxy mock:
- ~200 million galaxies
- over 5000 sq. deg
- up to a redshift z=1.4

We use:
- 10 samples
- 2 sq. deg.
- R_{ab}= 23 threshold magnitude
- up to a redshift z=0.8

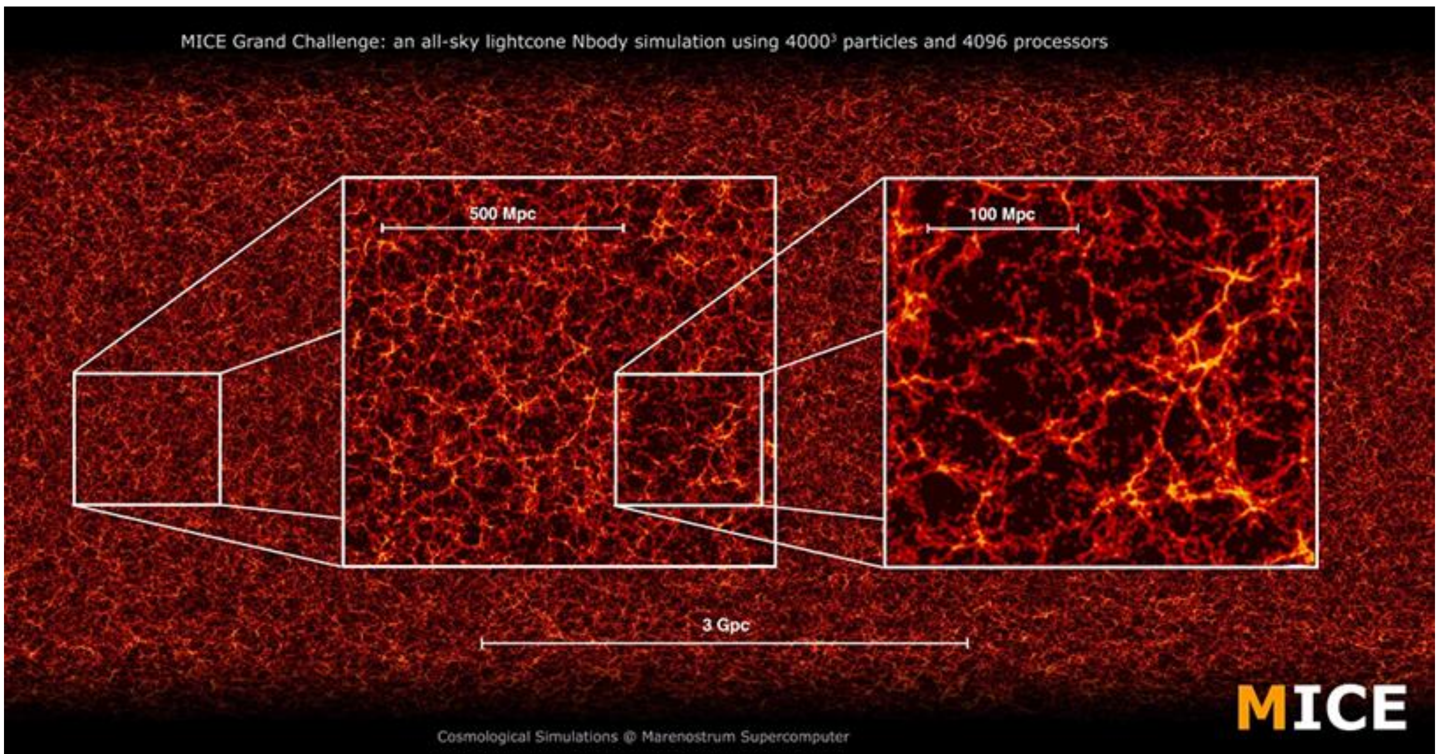

Fosalba et al. 2013a,b; Crocce et al. 2013; Castander et al. 2014; Carretero et al. 2014

Basic statistics

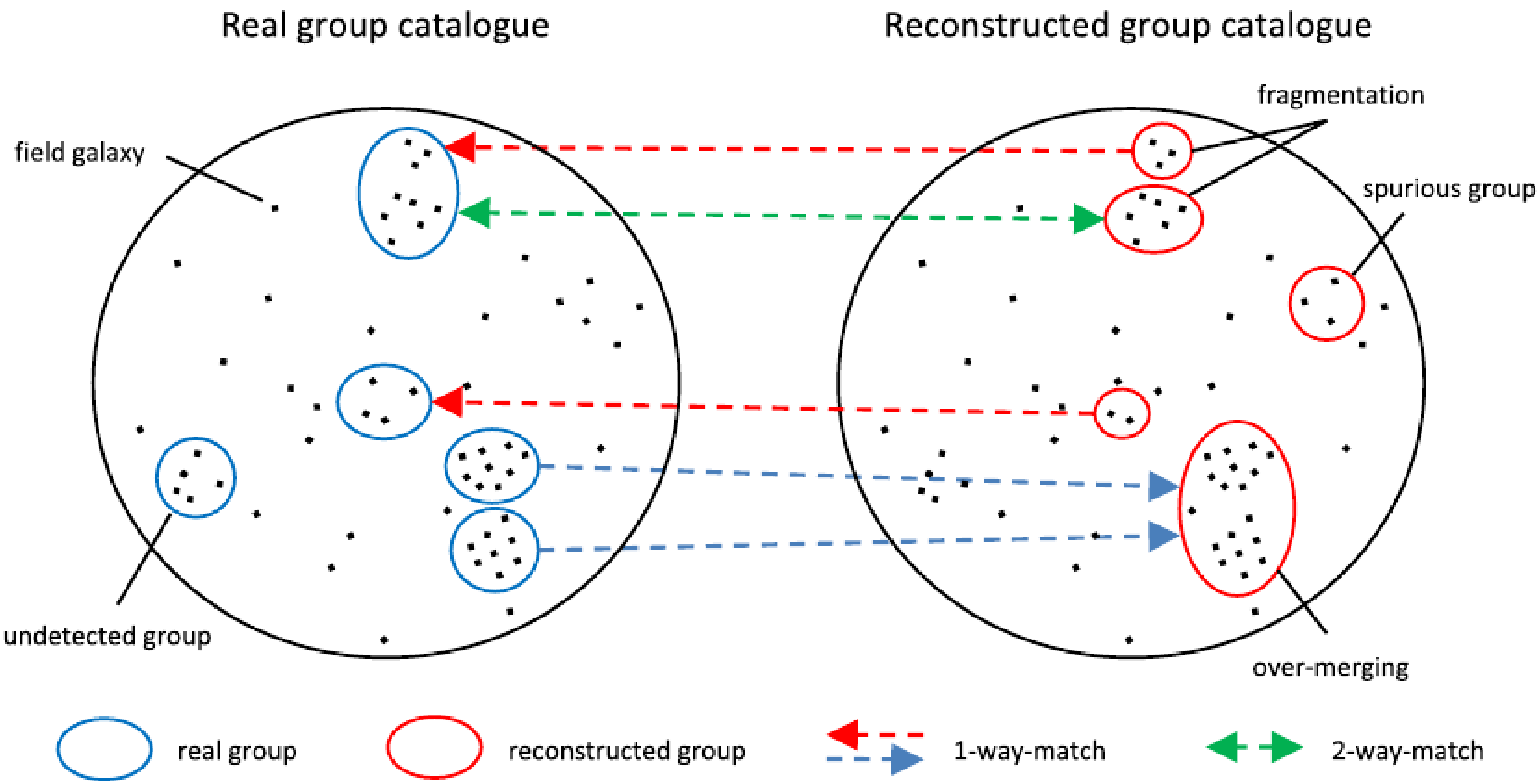

Knobel +,2010

Basic statistics

Completeness:

$$c_1 = \frac{N^{gr}_{real} \rightarrow N^{gr}_{rec}}{N^{gr}_{real}}, \quad c_2 = \frac{N^{gr}_{real} \leftrightarrow N^{gr}_{rec}}{N^{gr}_{real}}$$

Purity:

$$p_1 = \frac{N^{gr}_{rec} \rightarrow N^{gr}_{real}}{N^{gr}_{rec}}, \quad p_2 = \frac{N^{gr}_{rec} \leftrightarrow N^{gr}_{real}}{N^{gr}_{rec}}$$

Galaxy Success Rate:

$$S_{gal} = \frac{S^{gal}_{real} \cap S^{gal}_{rec}}{S^{gal}_{real}}$$

Interloper fraction:

$$f_I = \frac{S^{gal}_{rec} \cap S^{gal}_{field}}{S^{gal}_{rec}}$$

N^{gr}_{real} - the number of real groups, N^{gr}_{rec} - the number of reconstructed groups;
$N^{gr}_{real} \rightarrow N^{gr}_{rec}$ - the number of associations of real groups to reconstructed groups;
$N^{gr}_{rec} \rightarrow N^{gr}_{real}$- the number of associations of reconstructed groups to real groups;
S^{gal}_{real} - the set of galaxies associated to real groups;
S^{gal}_{rec} - the set of galaxies associated to reconstructed groups;
S^{gal}_{field} - the set of real field galaxies.

Knobel+, 2010

Filtering algorithm with adaptive kernel

Width of redshift slice: $\Delta z = 0.01 \cdot (1 + z) \pm 25\%$

Density of galaxies distribution:

$$\delta_i = \frac{s}{{}^{4}\!/_{3}\,\pi R^3}$$

where s is the number of the nearest neighbor, R is the distance for the nearest neighbor.

Mean density in slice:

$$\bar{\delta} = \frac{1}{n}\sum_{i=1}^{n} \delta_i\,,$$

where n is overall number of galaxies in slice.

Density contrast:

$$\sigma_i + 1 = {}^{(\delta_i - \bar{\delta})}\!/_{\bar{\delta}} + 1$$

Filtering algorithm with adaptive kernel. 2D

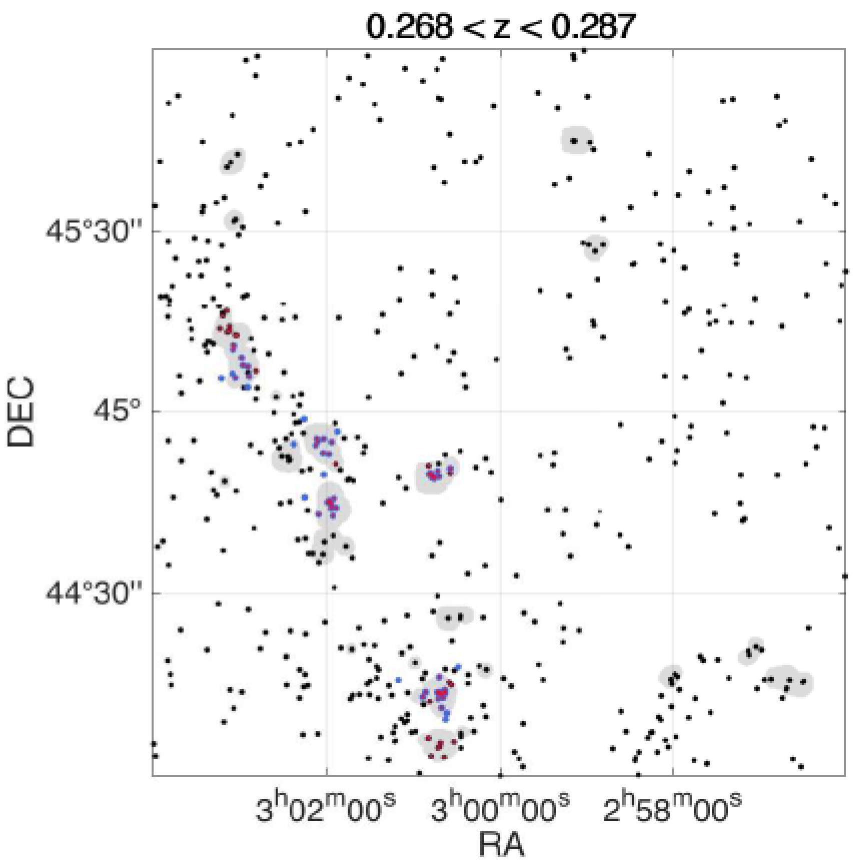

$N_{neighbor} = 2$

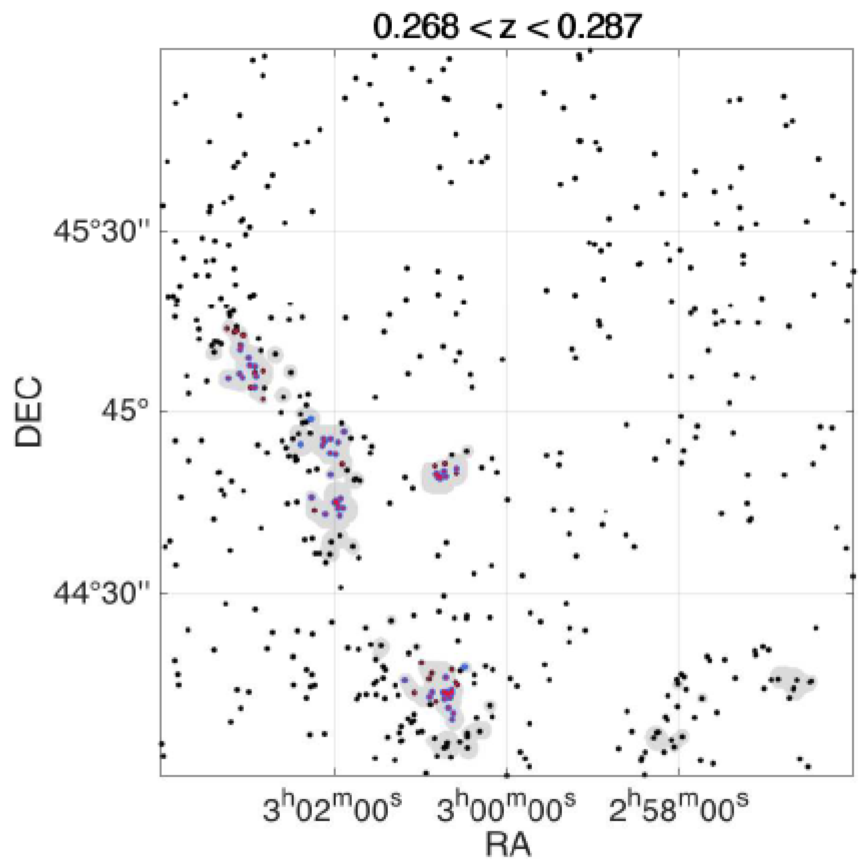

$N_{neighbor} = 5$

Filtering algorithm with adaptive kernel. 2D

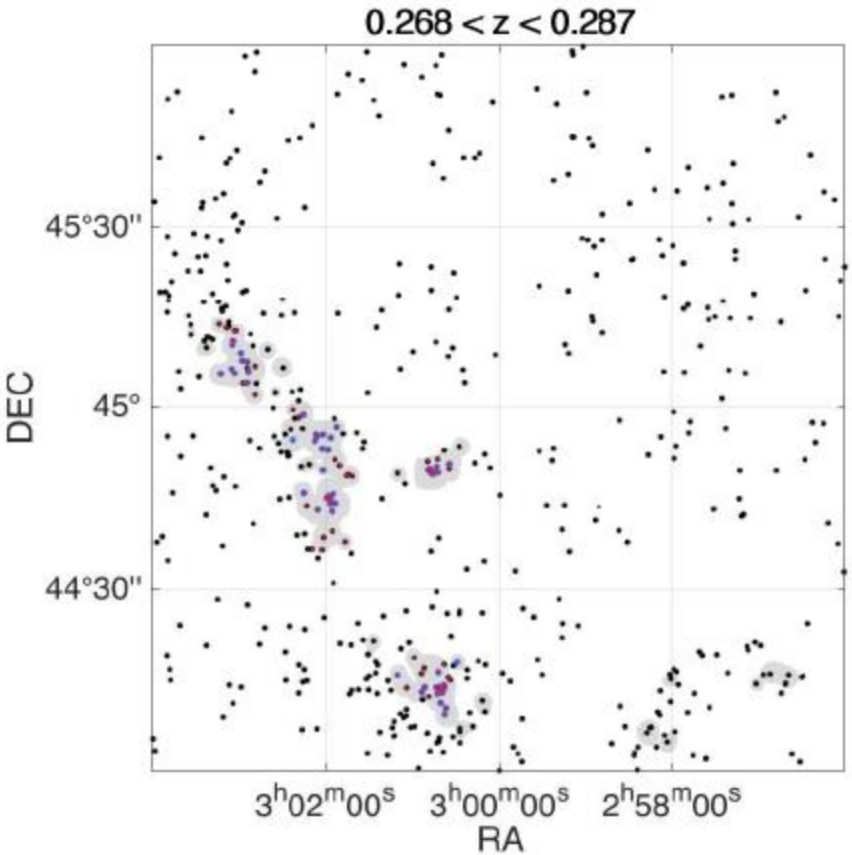

$N_{neighbor} = 7$

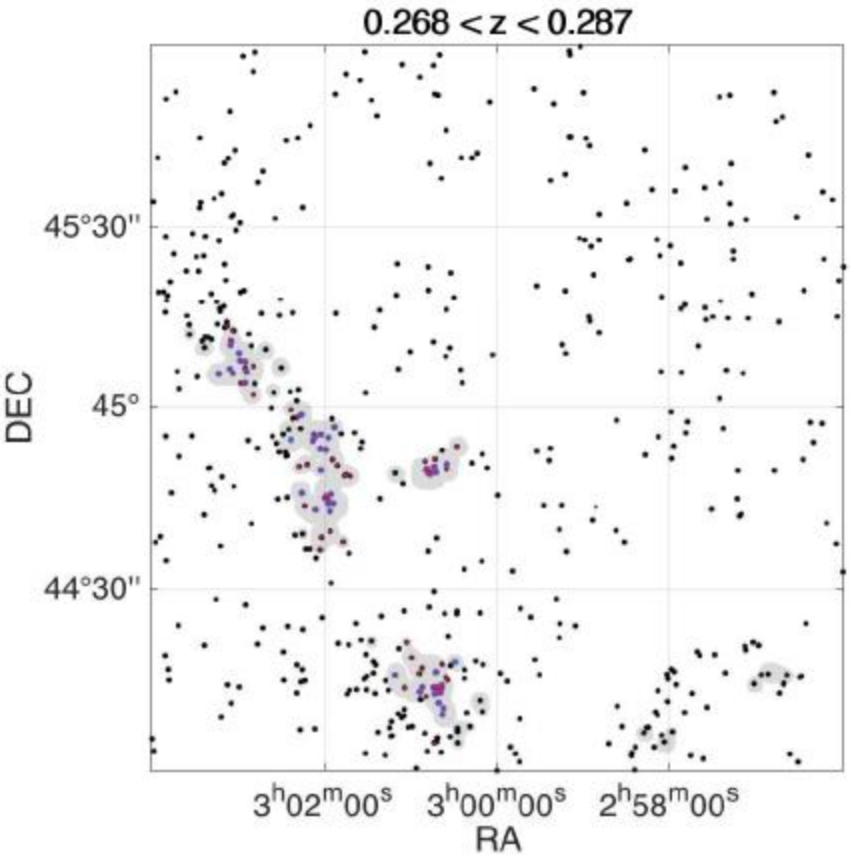

$N_{neighbor} = 8$

Filtering algorithm with adaptive kernel. 2D

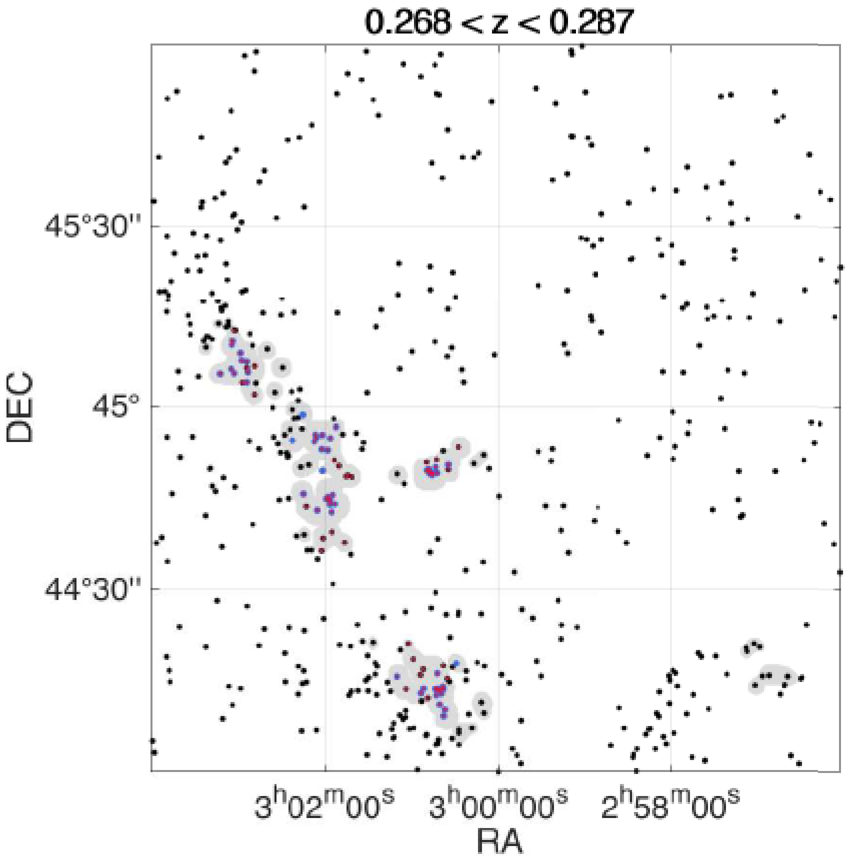

$N_{neighbor} = 10$

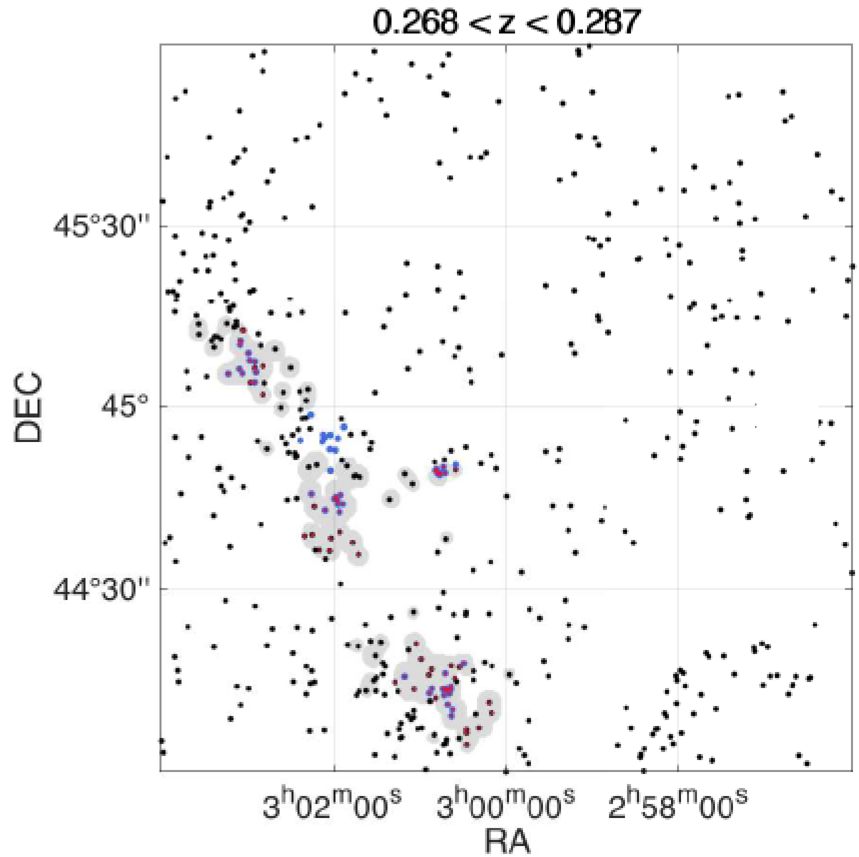

$N_{neighbor} = 20$

Filtering algorithm with adaptive kernel. 3D

0.268 < z < 0.287

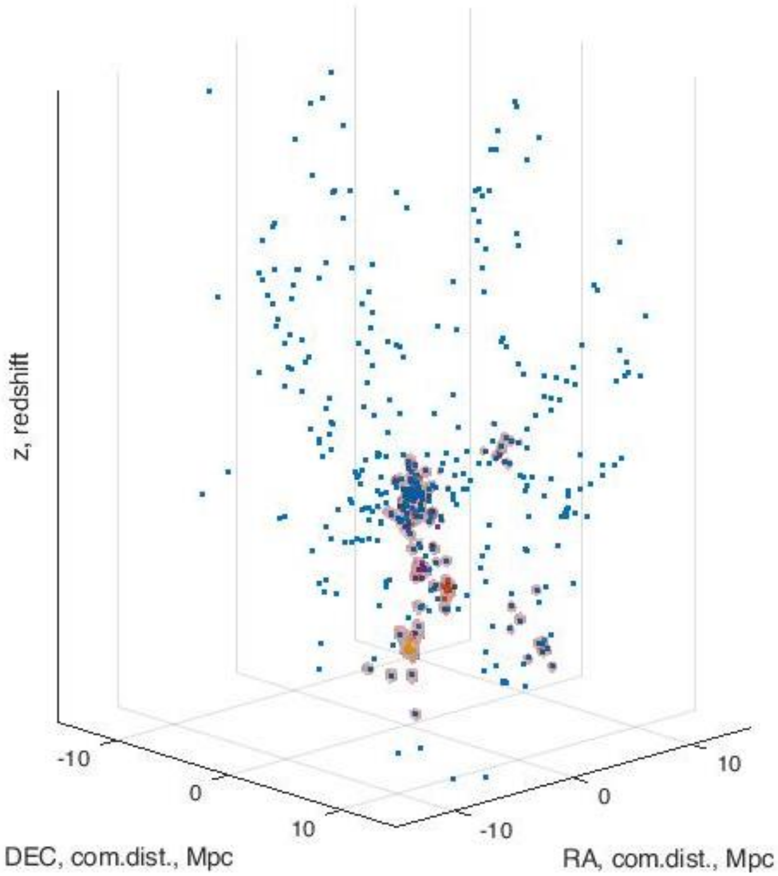

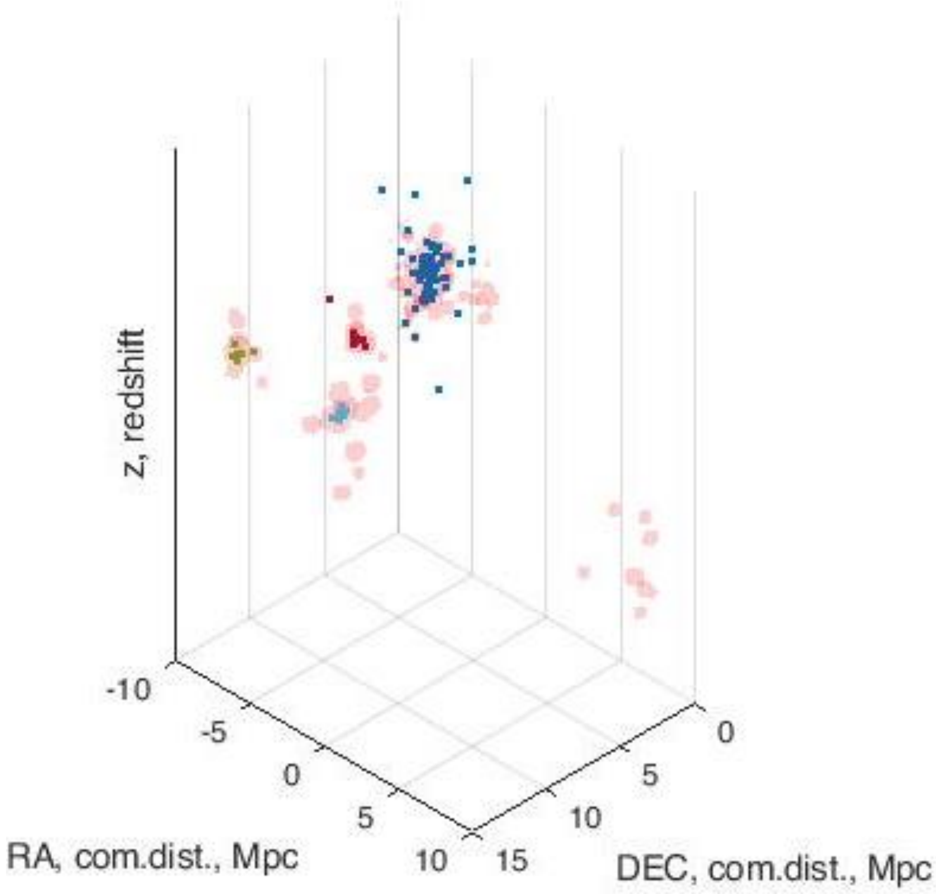

Study environmental dependence of galaxy properties
S. Dodonov, A. Grokhovskaya

Filtering algorithm with adaptive kernel. 3D

$0.268 < z < 0.287$

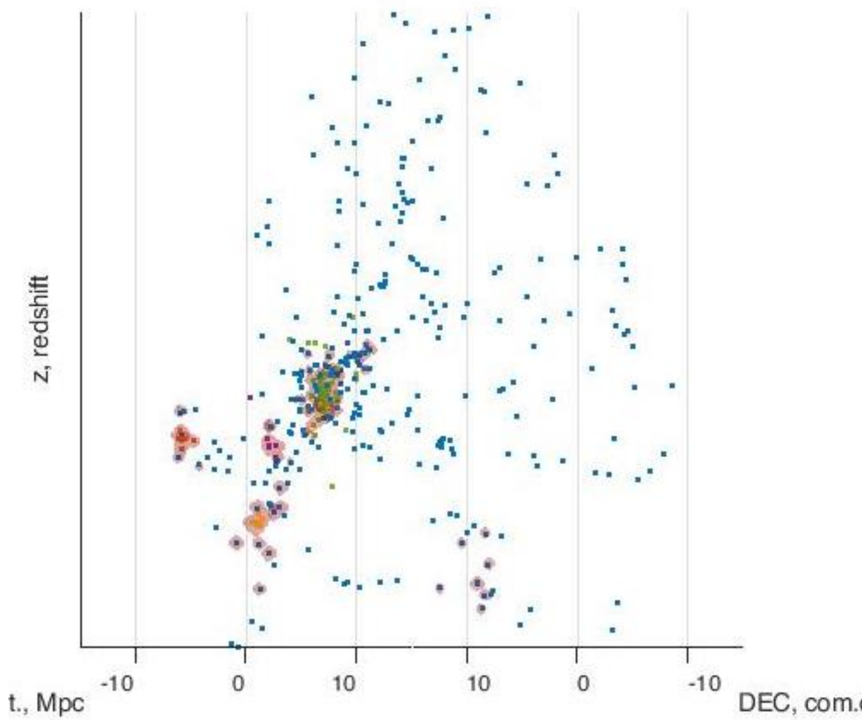

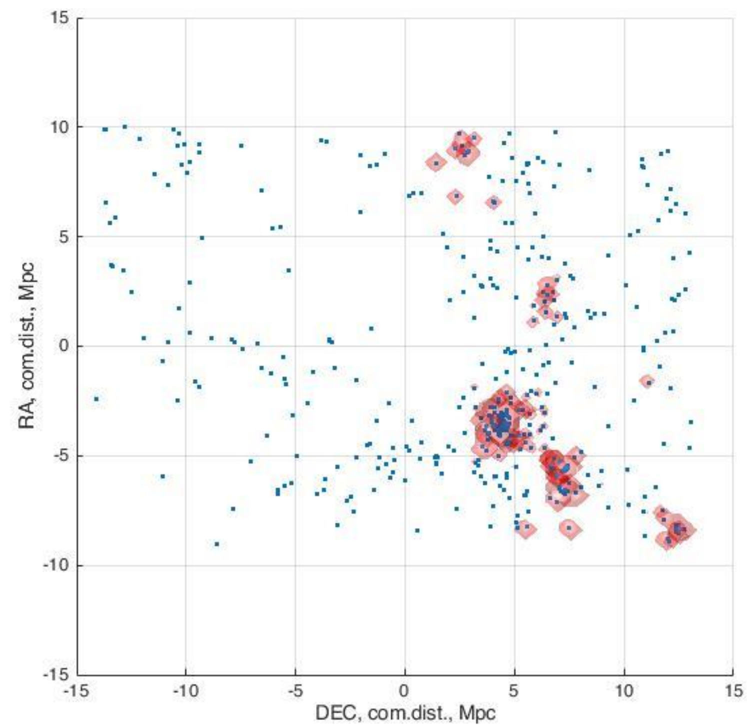

Study environmental dependence of galaxy properties
S. Dodonov, A. Grokhovskaya

Voronoi diagrams

Density contrast:

$$\sigma_i = {(\delta_i - \bar{\delta})}\Big/_{\bar{\delta}}$$

Mean density in slice:

$$\bar{\delta} = \frac{1}{n}\sum_{i=1}^{n}\frac{1}{A_i},$$

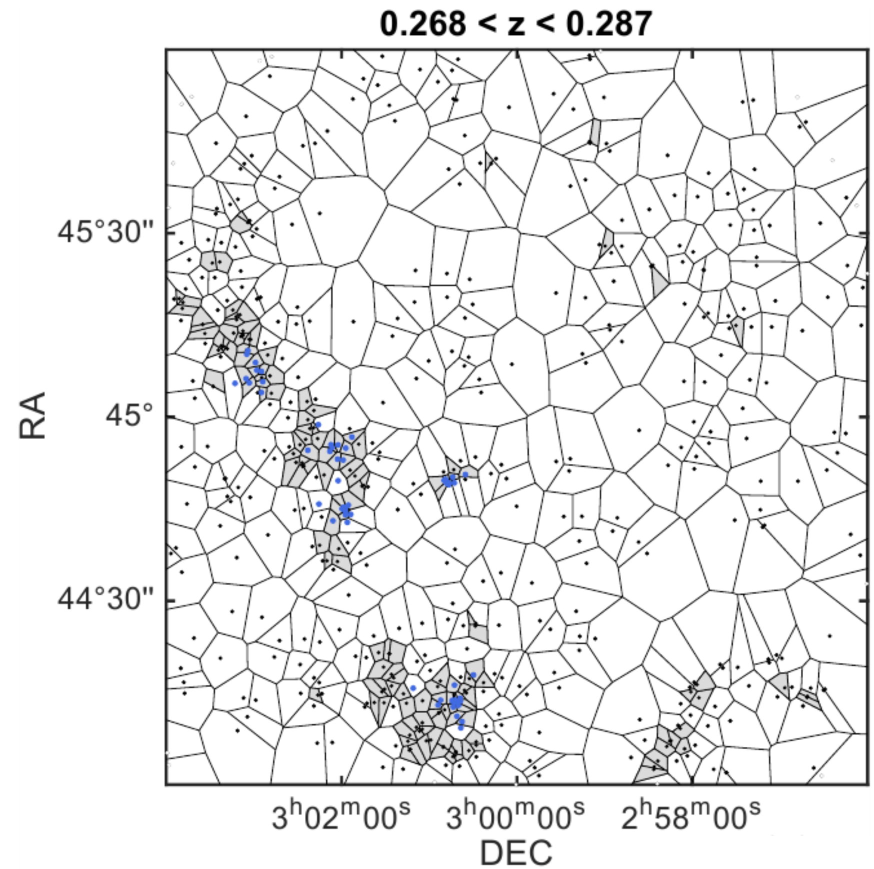

where $A_i -$ is the area of the Voronoi cell around object i and n is the overall number of objects.

Statistics for mock catalogs

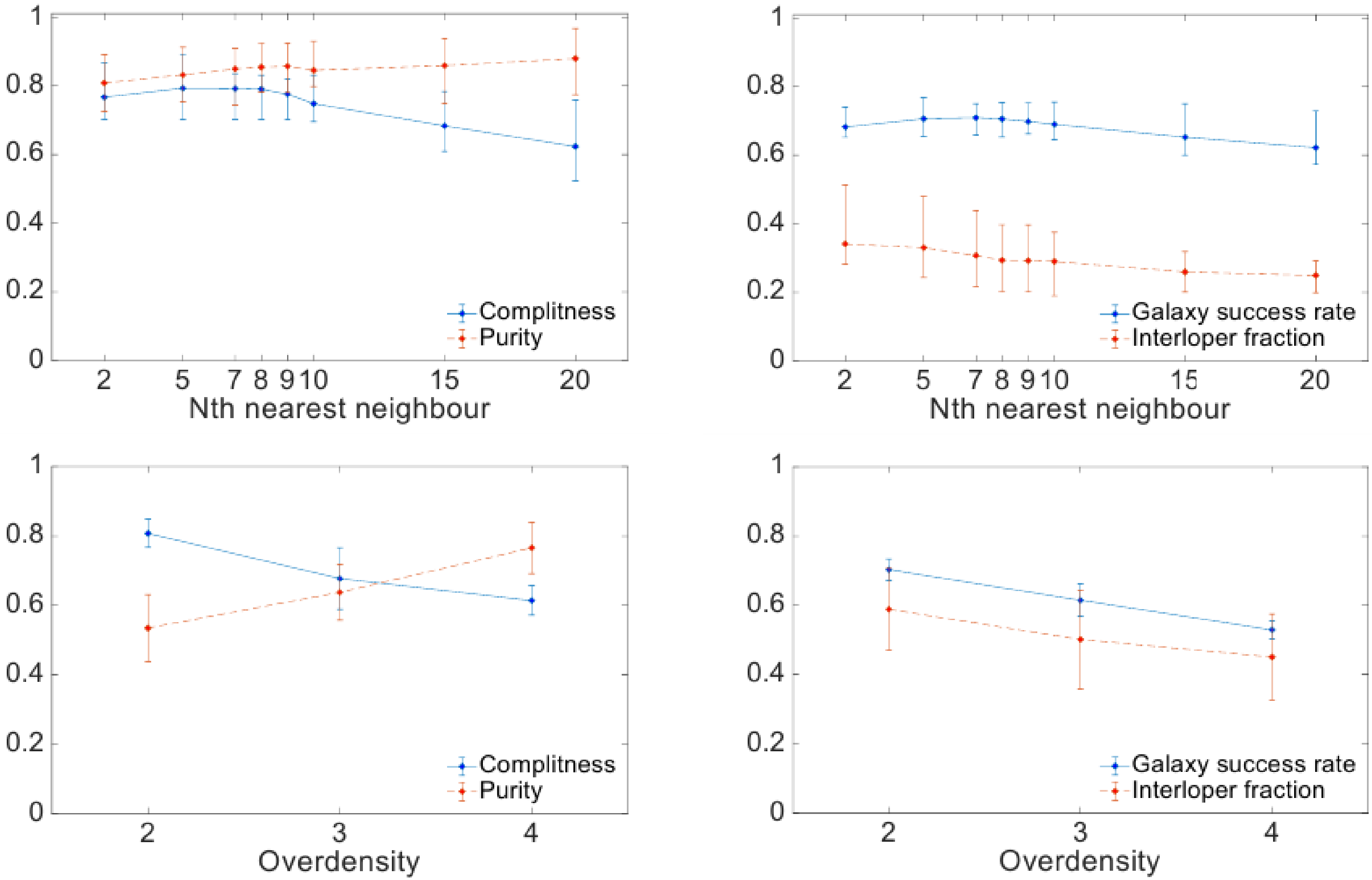

Filtering algorithm with adaptive kernel. 2D. HS 47.5 + 22 field

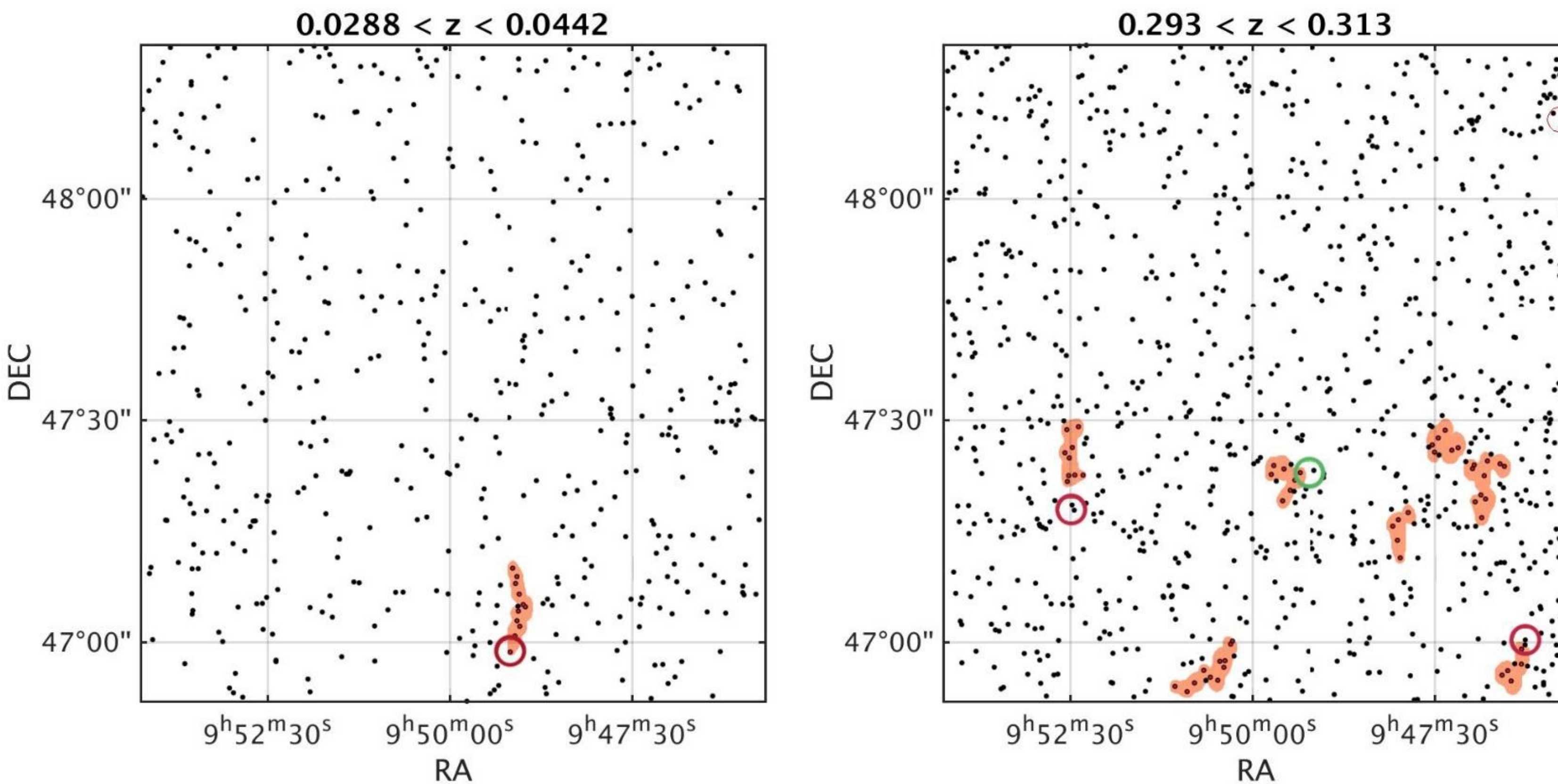

Filtering algorithm with adaptive kernel. 3D. HS 47.5 + 22 field

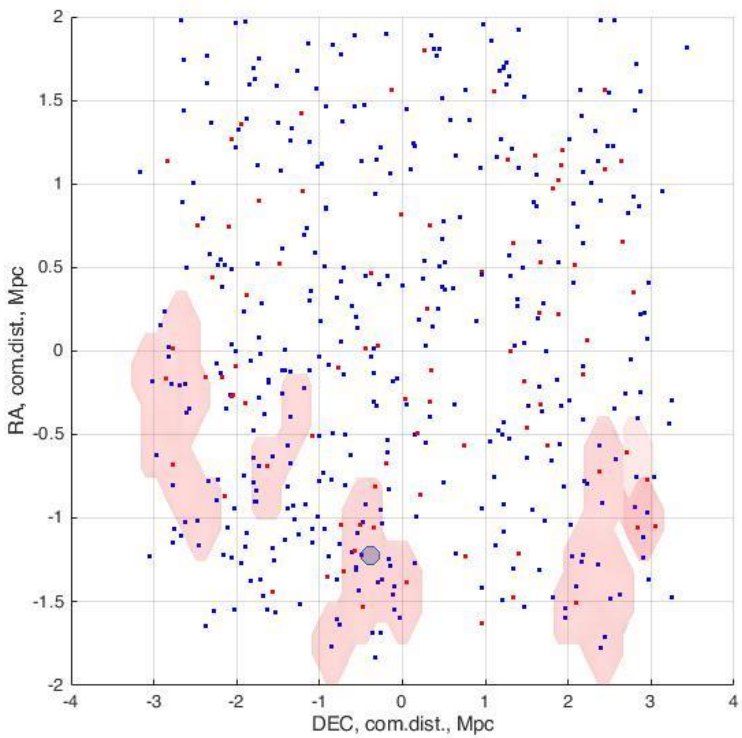

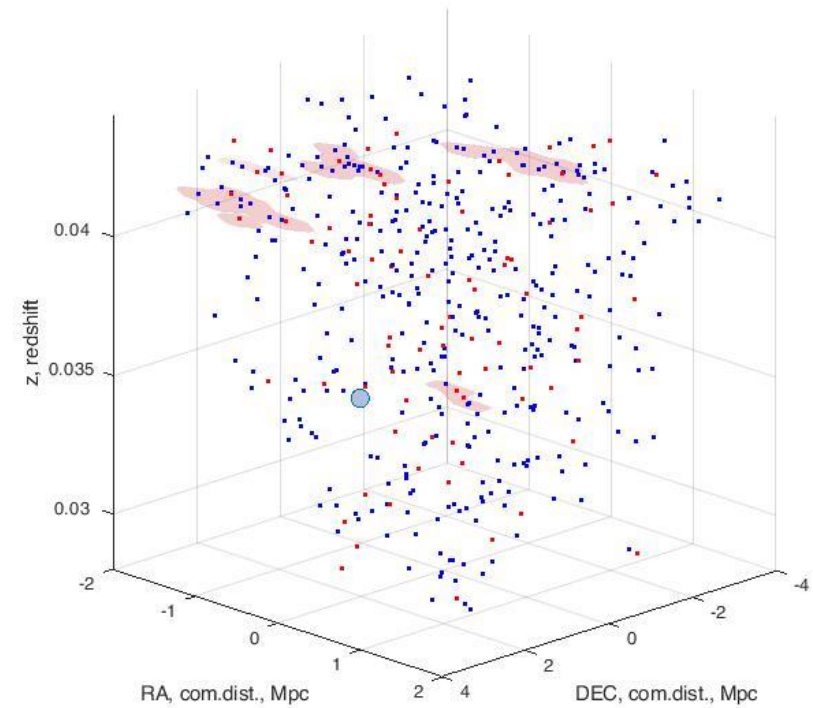

Detected cluster MSPM 01061 (Smith +, 2012)
z_{spec} = 0.03282

Conclusion

- We have tested multilateral analysis methods for large-scale distribution of galaxies.
- We explored the photometric properties of the sample of 36447 galaxies at the field HS47.5-22 and obtained spectral types and photometric redshifts for all objects.
- An accuracy of the redshift allows to determine an accessory of a galaxy to a cluster or a group.
- Based on the our photometric data we obtained maps of the contrast of density distribution with adaptive kernel algorithm (2D, 3D) and Voronoi tessellations (2D).

The main goal of our investigation is a study of the connection between star formation rate in galaxies and their position in the large scale distribution.